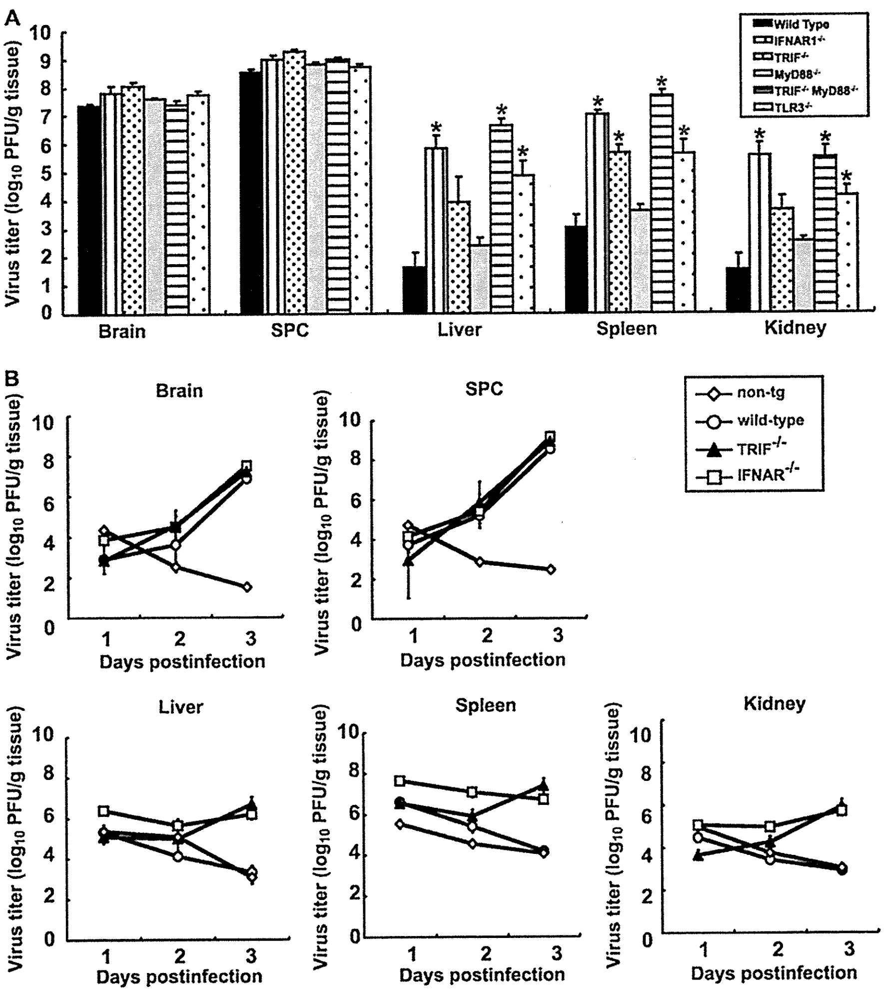

FIG 8 (A) PV replication in TRIF- and MyD88-deficient mice. Wild-type ($n = 4$), TRIF$^{-/-}$ ($n = 4$), MyD88$^{-/-}$ ($n = 6$), TRIF$^{-/-}$ MyD88$^{-/-}$ ($n = 4$), TLR3$^{-/-}$ ($n = 5$), and IFNAR1$^{-/-}$ ($n = 4$) mice were intravenously infected with 10^7 PFU of PV. The infected mice were paralyzed or dead at 3 to 5 days postinfection. The indicated tissues were collected, and viral titers were determined using a plaque assay (*, $P < 0.01$ by t test compared to wild-type mice). (B) PV replication kinetics in TRIF-deficient mice. Nontransgenic mice, wild-type mice, TRIF$^{-/-}$ mice, and IFNAR1$^{-/-}$ mice ($n = 3$) were infected as described above. Tissues were collected daily, and viral titers were determined. The results for nontransgenic (non-tg) mice, wild-type mice, and IFNAR1$^{-/-}$ mice are the same as those in Fig. 4B. SPC, spinal cord.

TABLE 2 PV antigens in TRIF- and MyD88-deficient mice

Organ or tissue	No. of PV antigen-positive mice/no. of mice tested			
	Wild type	TRIF$^{-/-}$	MyD88$^{-/-}$	TRIF$^{-/-}$ MyD88$^{-/-}$
Brain	6/6	8/8	9/9	6/6
Spinal cord	6/6	8/8	9/9	6/6
Heart	0/6	0/8	0/8	0/6
Lung	0/6	0/8	0/8	0/6
Liver	0/6	0/8	0/9	0/6
Kidney	0/6	0/8	2/9	0/5
Spleen	0/6	0/8	0/9	0/6
Pancreas	2/6	0/8	7/9	4/6
Intestine	0/6	0/8	0/9	0/6
Adipose tissue	0/6	2/8	2/9	3/6

mice were compared (Fig. 9). Approximately 25% of the TRIF$^{-/-}$ mice died after infection with 10^2 PFU of PV, and almost all of the mice died after infection with more than 10^3 PFU of PV (Fig. 9A). Approximately 20% and 60% of the MyD88$^{-/-}$ mice died after infection with 10^3 and 10^4 PFU of PV, respectively (Fig. 9B and C). TRIF$^{-/-}$ MyD88$^{-/-}$ mice were the most susceptible. In total, 70% of the mice died after infection with 10^2 PFU of PV (Fig. 9A). The mortality rate of TRIF$^{-/-}$ MyD88$^{-/-}$ mice was very close to that of IFNAR1$^{-/-}$ mice (19). The mortality rate of TLR3$^{-/-}$ mice was similar to that of TRIF$^{-/-}$ mice (Fig. 9D, E, and F). These results suggest that the TRIF-mediated and MyD88-mediated antiviral responses contribute to the host's defense against PV infection and that the TLR3-TRIF-mediated response has the most dominant effect.

DISCUSSION

Each virus infects different cell types and has a characteristic mode of replication. In mammalian hosts, several viral RNA sensors,

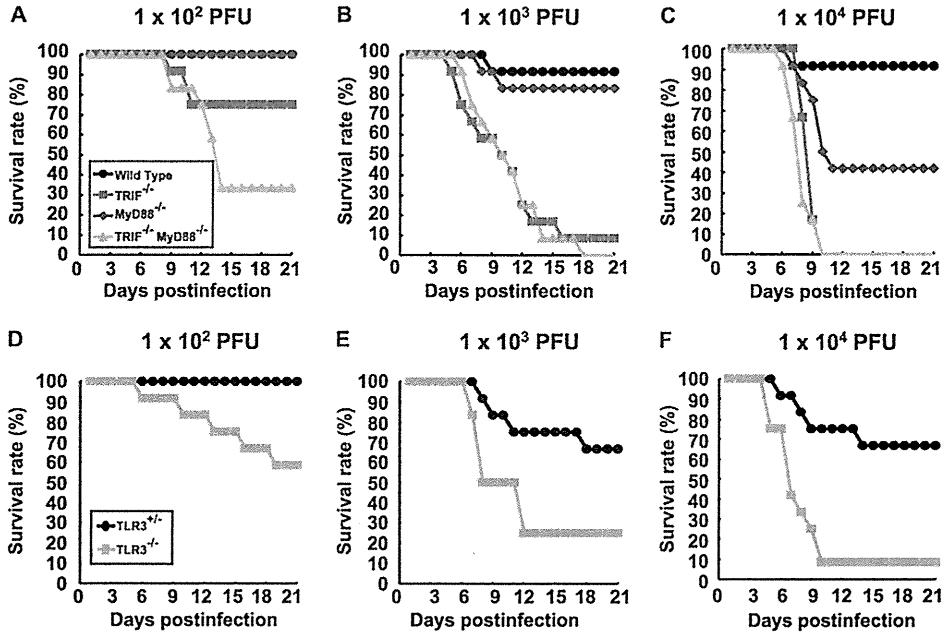

FIG 9 Mortality rates of TRIF-, MyD88-, and TLR3-deficient mice. (A) Wild-type, TRIF$^{-/-}$, MyD88$^{-/-}$, and TRIF$^{-/-}$ MyD88$^{-/-}$ mice (n = 12) were intravenously inoculated with the indicated doses of PV. (B) Littermates of TLR3$^{+/-}$ and TLR3$^{-/-}$ mice (n = 12) were used.

which are expressed in different cell types and recognize different molecular patterns, have evolved to counteract a variety of viruses. In the present study, we demonstrated that the MDA5-, TRIF-, and MyD88-mediated pathways contribute to the recognition of PV infection and that the TLR3-TRIF-mediated pathway plays the most important role in the antiviral response. Since all of the phenotypes shown after PV infection in the TRIF$^{-/-}$ mice and TLR3$^{-/-}$ mice are very similar to each other, we think that the contribution of the TLR3-mediated response is dominant and that of the TLR4-mediated response is negligible.

Previous reports have revealed that IFN is produced efficiently in EMCV-infected fibroblasts in an MDA5-dependent manner and that MDA5 contributes to the induction of serum IFNs and the protection of mice against EMCV (10, 23). Because EMCV belongs to the family *Picornaviridae*, we hypothesized that MDA5 also contributes to IFN induction in response to PV infection. However, the MDA5-dependent pathway did not play a dominant role in the defense against PV infection. Therefore, we speculate that PV uses mechanisms different from those of EMCV to strongly suppress IFN production *in vivo*. Indeed, IFN production in cultured cells in response to PV infection was observed only when the cells were pretreated with a low dose of IFNs. In addition, the amount of IFN produced was much lower than that produced in response to EMCV infection (Fig. 1). This result suggests that IFN induction in infected cells is suppressed and that this PV-mediated effect may be stronger than that of EMCV. Translational shutoff may be one of the reasons for this difference. PV 3A protein causes a change in membrane trafficking that prevents protein secretion and may also contribute to the suppression of IFN production (6). Caspase-dependent cleavage of MDA5 (3) and IPS-1 (39) in PV-infected cells has been reported. Through these possible mechanisms, PV may induce the suppression of IFN production in mice *in vivo*, and the MDA5-mediated pathway does not play an essential role in the host response, unlike in EMCV infection. PV and EMCV seemed to use different strategies to counteract the host innate immune system, even though PV and EMCV belong to the same family. Thus, TLR3 became the sensor that functions most effectively for PV as a result of PV evolution. Although the TLR3-TRIF-mediated pathway plays a dominant role, the fact that significant ISG induction was observed in PV-infected TRIF$^{-/-}$ and TRIF$^{-/-}$ MyD88$^{-/-}$ mice (Fig. 7) suggested that other mechanisms also operate in combination with this pathway.

The viral loads in the nonneural tissues of TLR3- and TRIF-deficient mice were much higher than those in wild-type mice, whereas the viral loads in the CNS were not significantly different in paralyzed mice (Fig. 8). These results suggest that the TLR3-TRIF-mediated pathway inhibits viral replication mainly before viral invasion of the CNS rather than after invasion and that this response plays an important role in preventing the viral invasion of the CNS. In the CNS, replication of PV was not effectively inhibited, even in wild-type mice. This result is consistent with our previous results obtained using IFNAR1$^{-/-}$ mice and suggests that the antivirus response in the CNS is different from that in nonneural tissues upon PV infection (19). The cell tropism of PV may influence the efficiency of the immune response. For example, if PVR is expressed in TLR3-expressing cells, then PV replication would be detected immediately after infection. Alternatively, if PV infection *in vivo* occurs in the vicinity of TLR3-expressing immune cells such as DCs and macrophages, PV-infected cells may readily be captured by TLR3-expressing cells, thereby facilitating efficient cross-priming (27, 44) of PV RNA. PV infects neurons almost exclusively and not other cell types in the CNS. If neurons do not have the ability to induce a strong TLR3-mediated antiviral response upon PV infection, the CNS may be more defective in the innate immune response than nonneural tissues are. This may be one of the reasons why PV replicates preferentially in the CNS. Further studies on PV pathogenesis related to the innate immune response will make a great contribution to elucidating the mechanisms of PV tissue tropism.

TLR3 recognizes dsRNA. However, the protective role of TLR3 in the response to many RNA viral infections is not clear (9, 29, 43). A previous study has demonstrated that WNV, which is an encephalitis virus belonging to the family *Flaviviridae*, causes more severe encephalitis in mice with intact TLR3 than in $TLR3^{-/-}$ mice. Peripheral WNV infection leads to a breakdown of the blood-brain barrier (BBB) and enhances brain infection in wild-type mice but not in $TLR3^{-/-}$ mice (50). In contrast, a protective role of the TLR3-mediated pathway in PV infection was clearly demonstrated in the present study. PV enters the CNS directly across the BBB via a PVR-independent mechanism (52) and from the neuromuscular junction via retrograde axonal transport (31–33). Because PV originally possesses two entry pathways into the CNS, the generation of a new entry pathway, even if it did occur, might not increase its deteriorative effect.

Interestingly, protective roles of the TLR3-mediated pathway have been reported for group B coxsackievirus (30, 41, 42), human rhinovirus (49), and EMCV (11) infections. Riad et al. (41) demonstrated that $TRIF^{-/-}$ mice showed severe myocarditis after CVB3 infection and IFN-β treatment improved virus control and reduced cardiac inflammation. Richer et al. (42) reported that $TLR3^{-/-}$ mice produced reduced proinflammatory mediators and were unable to control CVB4 replication at the early stages of infection, resulting in severe cardiac damage. They also showed that adoptive transfer of wild-type macrophages into $TLR3^{-/-}$ mice challenged with CVB4 resulted in greater survival, suggesting the importance of the TLR3-mediated pathway in the macrophage. Negishi et al. (30) reported that $TLR3^{-/-}$ mice showed vulnerability to CVB3 and that TLR3 signaling is linked to the activation of the type II IFN system. Since CVB3 does not induce robust type I IFNs, they suggested that the TLR3 type II IFN pathway serves as an "ace in the hole" in infections with such viruses. PV is similar to CVB3 because type I IFN production is low. However, in our preliminary experiments on PV infection in IFN-$\gamma^{-/-}$ PVR-tg mice, type II IFN did not make a significant contribution to the pathogenesis of PV. Taken together, these results suggest a critical role for the TLR3-mediated pathway, but the precise mechanisms leading to host protection are still controversial and the downstream events of TLR3 signaling after picornavirus infection remain to be elucidated.

Because the above-mentioned viruses are picornaviruses, picornavirus RNA may be easily detected by TLR3. There may be a common RNA structure in the genome or in the replication intermediates of these viruses that is detected by TLR3. Alternatively, picornaviral RNA may replicate in a compartment in which TLR3 can easily access the replicating dsRNA. To investigate these hypotheses, identification of the cells responsible for IFN production is an important step. Oshiumi et al. demonstrated that splenic $CD8\alpha^{+}$ $CD11c^{+}$ cells, bone marrow-derived macrophages, and DCs are able to elicit IFN in response to PV infection (35). Further studies using this virus-cell system will elucidate the molecular recognition pattern in the PV genome, the precise mechanism of PV RNA recognition in TLR3-expressing cells, and the roles of these cells in the prevention of PV dissemination in the body.

ACKNOWLEDGMENTS

We thank Takashi Fujita, Mitsutoshi Yoneyama, Hiroki Kato, Masahiro Yamamoto, Satoshi Uematsu, Seiya Yamayoshi, Akira Ainai, Hideki Hasegawa, and Takashi Kawanishi for helpful discussions and technical assistance.

This work was supported, in part, by Grants-in-Aid from the Ministry of Education, Culture, Sports, Science and Technology, Japan (Grants-in-Aid for Scientific Research on Priority Areas no. 21022053), and Grants-in-Aid for Research on Emerging and Re-emerging Infectious Diseases from the Ministry of Health, Labor and Welfare, Japan.

REFERENCES

1. **Akira S, Uematsu S, Takeuchi O.** 2006. Pathogen recognition and innate immunity. Cell **124**:783–801.
2. **Alexopoulou L, Holt AC, Medzhitov R, Flavell RA.** 2001. Recognition of double-stranded RNA and activation of NF-kappaB by Toll-like receptor 3. Nature **413**:732–738.
3. **Barral PM, et al.** 2007. MDA-5 is cleaved in poliovirus-infected cells. J. Virol. **81**:3677–3684.
4. **Bodian D.** 1959. Poliomyelitis: pathogenesis and histopathology, p 479–518. *In*Rivers TM, Horsfall FL, Jr (ed), Viral and rickettsial infections of man, vol 3. J. B. Lippincott, Philadelphia, PA.
5. **Cella M, et al.** 1999. Plasmacytoid monocytes migrate to inflamed lymph nodes and produce large amounts of type I interferon. Nat. Med. 5:919–923.
6. **Choe SS, Dodd DA, Kirkegaard K.** 2005. Inhibition of cellular protein secretion by picornaviral 3A proteins. Virology 337:18–29.
7. **Colonna M, Trinchieri G, Liu YJ.** 2004. Plasmacytoid dendritic cells in immunity. Nat. Immunol. 5:1219–1226.
8. **Diebold SS, Kaisho T, Hemmi H, Akira S, Reis e Sousa C.** 2004. Innate antiviral responses by means of TLR7-mediated recognition of single-stranded RNA. Science **303**:1529–1531.
9. **Edelmann KH, et al.** 2004. Does Toll-like receptor 3 play a biological role in virus infections? Virology 322:231–238.
10. **Gitlin L, et al.** 2006. Essential role of mda-5 in type I IFN responses to polyriboinosinic:polyribocytidylic acid and encephalomyocarditis picornavirus. Proc. Natl. Acad. Sci. U. S. A. **103**:8459–8464.
11. **Hardarson HS, et al.** 2007. Toll-like receptor 3 is an essential component of the innate stress response in virus-induced cardiac injury. Am. J. Physiol. Heart Circ. Physiol. **292**:H251–H258.
12. **Hemmi H, et al.** 2002. Small anti-viral compounds activate immune cells via the TLR7 MyD88-dependent signaling pathway. Nat. Immunol. 3:196–200.
13. **Hoebe K, et al.** 2003. Identification of Lps2 as a key transducer of MyD88-independent TIR signalling. Nature **424**:743–748.
14. **Holland JJ.** 1961. Receptor affinities as major determinants of enterovirus tissue tropisms in humans. Virology **15**:312–326.
15. **Holland JJ, Mc LL, Syverton JT.** 1959. Mammalian cell-virus relationship. III. Poliovirus production by non-primate cells exposed to poliovirus ribonucleic acid. Proc. Soc. Exp. Biol. Med. **100**:843–845.
16. **Holland JJ, McLaren LC, Syverton JT.** 1959. The mammalian cell-virus relationship. IV. Infection of naturally insusceptible cells with enterovirus ribonucleic acid. J. Exp. Med. **110**:65–80.
17. **Hornung V, et al.** 2006. 5′-Triphosphate RNA is the ligand for RIG-I. Science **314**:994–997.
18. **Hsiung GD, Black FL, Henderson JR.** 1964. Susceptibility of primates to viruses in relation to taxonomic classification, p 1–23. *In*Buettner-Jaenusch J (ed), Evolutionary and genetic biology of primates, vol 2. Academic Press, New York, NY.
19. **Ida-Hosonuma M, et al.** 2005. The alpha/beta interferon response controls tissue tropism and pathogenicity of poliovirus. J. Virol. **79**: 4460–4469.
20. **Ida-Hosonuma M, et al.** 2003. Host range of poliovirus is restricted to simians because of a rapid sequence change of the poliovirus receptor gene during evolution. Arch. Virol. **148**:29–44.
21. **Kato H, et al.** 2005. Cell type-specific involvement of RIG-I in antiviral response. Immunity 23:19–28.
22. **Kato H, et al.** 2008. Length-dependent recognition of double-stranded ribonucleic acids by retinoic acid-inducible gene-I and melanoma differentiation-associated gene 5. J. Exp. Med. **205**:1601–1610.
23. **Kato H, et al.** 2006. Differential roles of MDA5 and RIG-I helicases in the recognition of RNA viruses. Nature **441**:101–105.
24. **Koike S, et al.** 1992. A second gene for the African green monkey poliovirus receptor that has no putative N-glycosylation site in the functional N-terminal immunoglobulin-like domain. J. Virol. **66**:7059–7066.

25. **Koike S, Nomoto A.** 2010. Poliomyelitis, p 339–351. *In*Ehrenfeld E, Domingo E, Roos RP (ed), The picornaviruses. ASM Press, Washington, DC.
26. **Koike S, et al.** 1991. Transgenic mice susceptible to poliovirus. Proc. Natl. Acad. Sci. U. S. A. **88:**951–955.
27. **Kramer M, et al.** 2008. Phagocytosis of picornavirus-infected cells induces an RNA-dependent antiviral state in human dendritic cells. J. Virol. 82:2930–2937.
28. **Matsumoto M, et al.** 2003. Subcellular localization of Toll-like receptor 3 in human dendritic cells. J. Immunol. **171:**3154–3162.
29. **Matsumoto M, Oshiumi H, Seya T.** 2011. Antiviral responses induced by the TLR3 pathway. Rev. Med. Virol. **21:**67–77.
30. **Negishi H, et al.** 2008. A critical link between Toll-like receptor 3 and type II interferon signaling pathways in antiviral innate immunity. Proc. Natl. Acad. Sci. U. S. A. **105:**20446–20451.
31. **Ohka S, et al.** 2004. Receptor (CD155)-dependent endocytosis of poliovirus and retrograde axonal transport of the endosome. J. Virol. **78:** 7186–7198.
32. **Ohka S, et al.** 2009. Receptor-dependent and -independent axonal retrograde transport of poliovirus in motor neurons. J. Virol. **83:**4995–5004.
33. **Ohka S, Yang WX, Terada E, Iwasaki K, Nomoto A.** 1998. Retrograde transport of intact poliovirus through the axon via the fast transport system. Virology **250:**67–75.
34. **Oshiumi H, Matsumoto M, Funami K, Akazawa T, Seya T.** 2003. TICAM-1, an adaptor molecule that participates in Toll-like receptor 3-mediated interferon-beta induction. Nat. Immunol. **4:**161–167.
35. **Oshiumi H, et al.** 12 October 2011, posting date. The TLR3-TICAM-1 pathway is mandatory for innate immune responses to poliovirus infection. J. Immunol. [Epub ahead of print.] doi:10.4049/jimmunol.1101503.
36. **Pichlmair A, et al.** 2006. RIG-I-mediated antiviral responses to single-stranded RNA bearing 5′-phosphates. Science **314:**997–1001.
37. **Pichlmair A, et al.** 2009. Activation of MDA5 requires higher-order RNA structures generated during virus infection. J. Virol. **83:**10761–10769.
38. **Racaniello VR.** 2007. Picornaviridae: the viruses and their replication, p 795–838. *In*Knipe DM, Howley PM (ed), Fields virology, 5th ed. Lippincott Williams & Wilkins, Philadelphia, PA.
39. **Rebsamen M, Meylan E, Curran J, Tschopp J.** 2008. The antiviral adaptor proteins Cardif and Trif are processed and inactivated by caspases. Cell Death Differ. **15:**1804–1811.
40. **Ren RB, Costantini F, Gorgacz EJ, Lee JJ, Racaniello VR.** 1990. Transgenic mice expressing a human poliovirus receptor: a new model for poliomyelitis. Cell **63:**353–362.
41. **Riad A, et al.** 2011. TRIF is a critical survival factor in viral cardiomyopathy. J. Immunol. **186:**2561–2570.
42. **Richer MJ, Lavallee DJ, Shanina I, Horwitz MS.** 2009. Toll-like receptor 3 signaling on macrophages is required for survival following coxsackievirus B4 infection. PLoS One **4:**e4127.
43. **Schröder M, Bowie AG.** 2005. TLR3 in antiviral immunity: key player or bystander? Trends Immunol. **26:**462–468.
44. **Schulz O, et al.** 2005. Toll-like receptor 3 promotes cross-priming to virus-infected cells. Nature **433:**887–892.
45. **Shiroki K, et al.** 1995. A new *cis*-acting element for RNA replication within the 5′ noncoding region of poliovirus type 1 RNA. J. Virol. **69:** 6825–6832.
46. **Takeuchi O, Akira S.** 2009. Innate immunity to virus infection. Immunol. Rev. 227:75–86.
47. **Takeuchi O, Akira S.** 2008. MDA5/RIG-I and virus recognition. Curr. Opin. Immunol. **20:**17–22.
48. **Takeuchi O, Akira S.** 2007. Recognition of viruses by innate immunity. Immunol. Rev. 220:214–224.
49. **Wang Q, et al.** 2009. Role of double-stranded RNA pattern recognition receptors in rhinovirus-induced airway epithelial cell responses. J. Immunol. **183:**6989–6997.
50. **Wang T, et al.** 2004. Toll-like receptor 3 mediates West Nile virus entry into the brain causing lethal encephalitis. Nat. Med. **10:**1366–1373.
51. **Yamamoto M, et al.** 2003. Role of adaptor TRIF in the MyD88-independent Toll-like receptor signaling pathway. Science **301:**640–643.
52. **Yang WX, et al.** 1997. Efficient delivery of circulating poliovirus to the central nervous system independently of poliovirus receptor. Virology 229:421–428.
53. **Yoneyama M, et al.** 2004. The RNA helicase RIG-I has an essential function in double-stranded RNA-induced innate antiviral responses. Nat. Immunol. 5:730–737.
54. **Yoshikawa T, et al.** 2006. Role of the alpha/beta interferon response in the acquisition of susceptibility to poliovirus by kidney cells in culture. J. Virol. **80:**4313–4325.
55. **Yousefi S, Escobar MR, Gouldin CW.** 1985. A practical cytopathic effect/dye-uptake interferon assay for routine use in the clinical laboratory. Am. J. Clin. Pathol. **83:**735–740.

RESEARCH PAPER
OncoImmunology 1:5, 1–12; September/October 2012; © 2012 Landes Bioscience

Cross-priming for antitumor CTL induced by soluble Ag + polyI:C depends on the TICAM-1 pathway in mouse CD11c+/CD8a+ dendritic cells

Masahiro Azuma, Takashi Ebihara,† Hiroyuki Oshiumi, Misako Matsumoto and Tsukasa Seya*

Department of Microbiology and Immunology; Hokkaido University Graduate School of Medicine; Sapporo, Japan

†Current address: Howard Hughes Medical Institute; Washington University School of Medicine; St. Louis, MO USA

Keywords: cross-presentation, dendritic cell, TLR3, TICAM-1 (TRIF), tumoricidal CTL

Abbreviations: APC, antigen-presenting cells; CTL, cytotoxic T lymphocytes; DAMP, damage-associated molecular pattern; DC, dendritic cells; IFN, interferon; IPS-1, IFN promoter stimulator-1; MDA5, melanoma differentiation associated gene 5; Mf, macrophages; NK, natural killer; OVA, ovalbumin; PAMP, pathogen-associated molecular pattern; PRR, pattern-recognition receptors; PV, poliovirus; RIG-I, retinoic acid inducible gene-1; SL8, an OVA tetramer; TICAM-1, Toll-IL-1 receptor homology domain-containing molecule-1; TLR, toll-like receptor; WT, wild-type

PolyI:C is a nucleotide pattern molecule that induces cross-presentation of foreign Ag in myeloid dendritic cells (DC) and MHC class I-dependent proliferation of cytotoxic T lymphocytes (CTL). DC (BM or spleen CD8a+) have sensors for dsRNA including polyI:C to signal facilitating cross-presentation. Endosomal TLR3 and cytoplasmic RIG-I/MDA5 are reportedly responsible for polyI:C sensing and presumed to deliver signal for cross-presentation via TICAM-1 (TRIF) and IPS-1 (MAVS, Cardif, VISA) adaptors, respectively. In fact, when tumor-associated Ag (TAA) was simultaneously taken up with polyI:C in DC, the DC cross-primed CTL specific to the TAA in a syngenic mouse model. Here we tested which of the TICAM-1 or IPS-1 pathway participate in cross-presentation of tumor-associated soluble Ag and retardation of tumor growth in the setting with a syngeneic tumor implant system, EG7/C57BL6, and exogenously challenged soluble Ag (EG7 lysate) and polyI:C. When EG7 lysate and polyI:C were subcutaneously injected in tumor-bearing mice, EG7 tumor growth retardation was observed in wild-type and to a lesser extent IPS-1$^{2/2}$ mice, but not TICAM-1$^{2/2}$ mice. IRF-3/7 were essential but IPS-1 and type I IFN were minimally involved in the polyI:C-mediated CTL proliferation. Although both TICAM-1 and IPS-1 contributed to CD86/CD40 upregulation in CD8a+ DC, H2K^b-SL8 tetramer and OT-1 proliferation assays indicated that OVA-recognizing CD8 T cells predominantly proliferated in vivo through TICAM-1 and CD8a+ DC is crucial in ex vivo analysis. Ultimately, tumor regresses . 8 d post polyI:C administration. The results infer that soluble tumor Ag induces tumor growth retardation, i.e., therapeutic potential, if the TICAM-1 signal coincidentally occurs in CD8a+ DC around the tumor.

Introduction

Cytotoxic T lymphocytes (CTL) and natural killer (NK) cells are two major effectors for antitumor cellular immunity. These effectors are driven through activation of dendritic cells (DC) and/or macrophages (Mf), which is mediated by pattern-recognition receptors (PRRs) for the recognition of microbial patterns.[1,2] Antigen (Ag) presentation and upregulation of NK cell-activating ligands are major events induced in DC/Mf in response to PRRs, which link to evoking CTL- and NK-antitumor immunity, respectively. The immune-potentiating function of specific components of the classical adjuvants are largely attributable to the ligand activity of PRRs (CpG DNA/TLR9, polyI:C/TLR3, monophosphoryl lipid (MPL) A/TLR4, Pam2/TLR2, etc.).[3] That is, the DC/Mf competent to drive effectors are generated through PRR signal in inflammatory nest where affected cells and recruited immune cells encounter exogenous or endogenous PRR ligands. Since studying the functional properties of PRRs in tumor immunity is on the way using a variety of possible ligands and cell biological analyses, immune responses reflecting the total adjuvant potential around Ag-presenting cells (APC) in local inflammatory nests are not always elucidated even in mice.

RNA-sensing PRR pathways, including TLR3-TICAM-1, TLR7-MyD88 and RIG-I/MDA5-IPS-1 participate in driving type I IFN induction and cellular immunity in DC subsets.[1,4,5] Type I IFN and the IFNAR pathway in DC and other cells reportedly evoke and amplify T cell immunity.[5,6] TLR7 resides exclusively in plasmacytoid DC[7] whereas TLR3 mainly exists in

*Correspondence to: Tsukasa Seya; Email: seya-tu@pop.med.hokudai.ac.jp
Submitted: 02/04/12; Revised: 03/02/12; Accepted: 03/02/12
http://dx.doi.org/10.4161/onci.19893

myeloid DC/Mf and epithelial cells.[8] They are localized on the membrane of the endosome and deliver the signal via their adaptors, MyD88 and TICAM-1.[7,8] RIG-I and MDA5 are ubiquitously distributed to a variety of mouse cells and signal the presence of cytoplasmic viral products through IPS-1.[9] Thus, TLR3 and RIG-I/MDA5 are candidates associated with DC maturation to drive effector cells.[10] Indeed, viral dsRNA analog, polyI:C, is a representative ligand for TLR3 and MDA5 and induces polyI:C-mediated DC-NK reciprocal activation.[11,12] These are also true in human DC.[13]

The point of this study is by which pathway antitumor CTL are induced for tumor regression in a mouse tumor-implant model. It has been postulated that DC present exogenous tumor Ag to the MHC class I-restricted Ag-presentation pathway and proliferate CD8 T cells specific to the extrinsic Ag. When tumor cells provide soluble and insoluble exogenous Ag, this class I Ag presentation occurs mostly TAP/proteasome-dependent, suggesting the pathway partly sharing with that for endogenous Ag presentation. This DC's ability to deliver exogenous Ag to the pathway for MHC class I-restricted Ag presentation has been described as cross-presentation.[14] DC cross-presentation leads to the cross-priming and proliferation of Ag-specific CD8 T cells in vivo and in vitro.[14-18] A variety of PAMP[15,16] and intrinsic DAMP[17] as well as other factors including type I IFN,[5,18] $CD4^+$ T cells[19] and NKT cells[20] augment cross-priming in tumor-bearing mice. However, by what molecular mechanism polyI:C enhances CTL induction in tumor-bearing mice remains largely unsettled.

Here, we made an EG7 tumor-implant mouse system and treated the mice with s.c.-injected ovalbumin (OVA)-containing cell lysates (Ag) and polyI:C. Spleen $CD8a^+$ DC turn CTL-inducible when stimulated with Ag and polyI:C. In either case of s.c., i.p., or i.v. injection of polyI:C, the TLR3/TICAM-1 pathway predominantly participates in $CD8a^+$ DC cross-priming and antitumor CTL induction. Earlier studies using non-tumor models, suggested that both TLR3 and MDA5 appeared to participate in polyI:C-dependent CTL induction.[21] TLR3 is predominantly involved in primary Ag response and Thl skewing,[22] while MDA5 participates in secondary Ag response.[23] Importance of TLR3 in induction of cross-priming was first suggested by Schulz et al., who used OVA/polyI:C-loaded or virus-infected xenogenic (Vero) cells and mouse DC.[16] Here we demonstrate that the antitumor polyI:C activity is sustained by the TICAM-1 pathway in any route of injection in tumor-implant mice: antitumor CTL responses are mostly abrogated in TICAM-1 $^{2/2}$ but not IPS-1 $^{2/2}$ mice.

Results

Properties of EG7 tumor with high MHC in tumor-loading mice. The properties of the EG7 line we used are consistent with those reported previously.[24,25] It expressed high MHC class I (H2-Kb) and no Qa-1b or Rae-1 (Fig. S1). The expression levels of these proteins were barely changed before and after implantation of EG7 cells into mice. Cell viability was not affected by in vitro stimulation with polyI:C only (Fig. S1B). However, a batch-to-batch difference of cell viability may have affected the rate of tumor growth in each mouse tumor-implant experiment.

$CD8^+$ T cells are responsible for tumor retardation by polyI:C. EG7 cells (2 10^6) were inoculated into the back of C57BL/6 (WT), and the indicated reagents were subcutaneously (s.c.) injected around the EG7 tumor (Fig. 1A). Growth retardation of tumor was observed by treatment with polyI:C or polyI:C plus EG7 lysate (Fig. 1A). EG7 lysate only had no effect on tumor regression. When CD8 $^+$ T cells were depleted before EG7 lysate/polyI:C treatment, polyI:C-mediated tumor growth suppression was cancelled (Fig. 1A), suggesting the participation of CD8 T cells in tumor growth suppression. The therapeutic potential of polyI:C appeared to be more reproducible in the presence of EG7 lysate than in the absence, judged from the increases of activated $CD8^+$ T cells (Fig. 1B) and cytotoxic activity (Fig. 1C) of LN T cells isolated from the mice sacrificed after the last therapy. Yet, the EG7 Ag could be more or less supplied from the implant tumor. $NK1.1^+$ cells did not participate in this EG7 tumor regression in this setting (data not shown).

Since EG7 lysate contains OVA, OVA-specific T cells in draining LN and spleen of the WT mice were counted by tetramer assay after the last therapy (Fig. S2A, B). The numbers of tetramer-positive cells were prominently increased in LN and spleen in mice with EG7 lysate and polyI:C. We confirmed the importance of simultaneous administration of Ag plus polyI:C for OVA-specific CTL induction as in Figure S2C, where pure Ag (OVA) was used instead of EG7 lysate for immunotherapy. The polyI:C adjuvant function appeared to be more efficient in the mixture of pure Ag than in polyI:C alone. Tumor regression (Fig. S2C) and OVA-specific CTL induction (Fig. S2D) were clearly observed in this additional experiment. To obtain reproducible data, we employed the EG7 lysate/polyI:C combination therapy as follows.

IFN-inducing pathways are involved in PolyI:C-derived EG7 growth retardation. We next inoculated EG7 cells (2 10^6) into the back of C57BL/6 (WT), TICAM-1 $^{2/2}$, IPS-1 $^{2/2}$, or TICAM-1/IPS-1 double-deficient (DKO) mice (Fig. 2). We s.c. administered EG7 lysate with or without polyI:C around the tumor. The EG7 lysate was the soluble fraction of EG7 which removed insoluble debris by centrifugation. The EG7 lysate contained unprecipitated micro-debris and soluble Ag. No other emulsified reagent was added for immunization. Thus, the adjuvant function of polyI:C per se is reflected in the tumor growth, although polyI:C had to be injected into mice twice a week. Retardation of tumor growth was observed . 8 d after immunization with EG7 lysate + polyI:C in WT mice, though no growth retardation without polyI:C (Fig. 2A). The polyI:C-mediated tumor growth suppression was largely abrogated in TICAM-1 $^{2/2}$ (Fig. 2B) and to a lesser extent in IPS-1 $^{2/2}$ mice (Fig. 2C), and completely in TICAM-1/IPS-1 DKO mice (Fig. 2D). Hence, TICAM-1 plays an important role in inducing polyI:C-mediated tumor growth retardation in the s.c. setting we employed.

CD8 T cell activation induced by the TICAM-1 pathway. CD8 T cell activation in the inguinal LN was tested with polyI:C + EG7 lysate in EG7 tumor-bearing mice using CD69 as

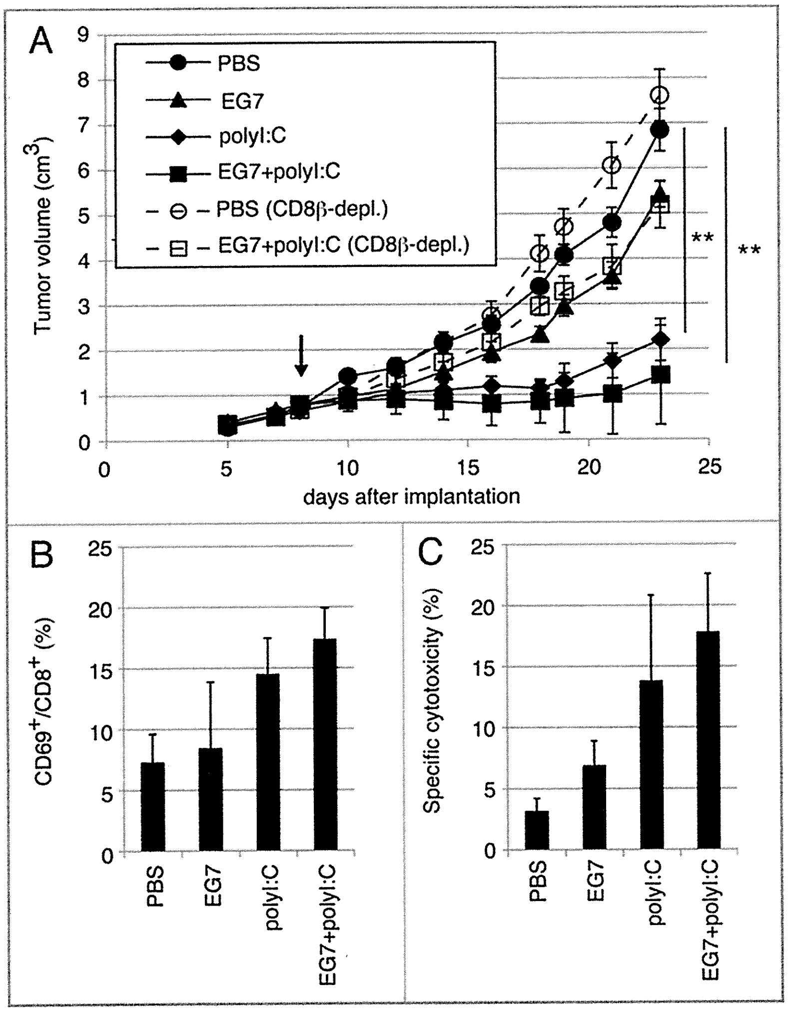

Figure 1. PolyI:C induces CTL-mediated tumor regression. (A) WT mice were challenged with EG7 cells and were treated with PBS( ), EG7 lysates( ), polyI:C ( ) and EG7 lysates + polyI:C( ). The adjuvant therapy was started at the time indicated by the arrow and the indicated reagents injected twice per week. One of the two PBS groups ( ) and one of the two EG7 lysates + polyI:C groups ( ) were treated with anti-CD8b ascites in order to deplete CD8⁺ T cells once a week. Each group had 3–5 mice. (B) Draining inguinal LNs were harvested 24 h after the last treatment and the proportion of CD69-expressing CD8⁺ cells were counted. (C) LN cells were co-cultured with MMC-treated EG7 cells for 3 d and subjected to ^{51}Cr release assay to evaluate CTL activity. E/t = 50. All error bars used in this figure show ± SEM. Data are representative of two independent experiments. One-way analysis of variance (ANOVA) with Bonferroni's test was performed to analyze statistical significance. **: p , 0.01.

an activating marker. Twenty-four h after the last polyI:C + EG7 sec.c. treatment, cells were harvested from the LN excised (Fig. 3A). FACS profiles of total cells from each mouse group are shown in Fig. S3. By combination therapy with EG7 lysate and polyI:C, T cells were activated in WT and IPS-1$^{2/2}$ mice, but the proportion of CD8 T cells was not affected by the therapy (Fig. S4A). Under the same conditions, T cells were barely activated in TICAM-1$^{2/2}$ mice in response to polyI:C (Fig. 3A). The proportion of CD69⁺ cells are indicated in Figure 3B. IL-2 (Fig. 3C) and IFN-c (Fig. S4B) were highly induced in the WT and IPS-1$^{2/2}$ LN cells, while they were not induced in TICAM-1$^{2/2}$ or DKO cells. IFN-c levels were upregulated only in polyI:C-treated tumor-bearing mice, although the WT . IPS-1$^{2/2}$ profile for IFN-c production was reproducibly observed (Fig. S4B).

In vivo proliferation of CD8 T cells judged by tetramer assay and IFN-c induction. We next tested whether i.p. injection of polyI:C plus OVA induces CTL proliferation. PolyI:C and OVA were i.p. injected into mice and the polyI:C-dependent cross-priming of CD8 T cells were examined using the OVA tetramer assay. OVA-specific CD8 T cells were clonally proliferated in WT and IPS-1$^{2/2}$ mice, but not in TICAM-1/IPS-1 DKO and IRF-3/7$^{2/2}$ mice (Fig. 4A). Proliferation of OVA-specific CD8 T cells were severely suppressed in TICAM-1$^{2/2}$ mice (Fig. 4A), suggesting that polyI:C-mediated cross-priming of CD8 T cells largely depends on the TICAM-1 pathway followed by IRF-3/7 activation in the i.p. route. The results were reproduced in additional experiments using more mice (Fig. 4B) and TLR3$^{2/2}$ mice (Fig. S5A,B). The polyI:C cytokine response, where IFN-a is IPS-1-dependent while IL-12p40 is TICAM-1-dependent, was also confirmed in serum level by polyI:C i.p. injection (Fig. S5E). Specific induction of IFN-c (Fig. 4C) was also observed in parallel with the results of Figure 4A.

Whether or not i.v. injection of polyI:C plus OVA induces Ag-specific CTL and cytotoxicity was next checked. OVA-specific OT-1 proliferation and cytotoxicity (Fig. 4D, E) were observed in in vivo analyses of WT and IPS-1$^{2/2}$ CD8 T cells but not of TICAM-1$^{2/2}$, TICAM-1/IPS-1 DKO, and IRF-3/7$^{2/2}$ mice in the i.v. setting.

Since TICAM-1 is the adaptor for TLR3 as well as cytoplasmic helicases,24 we confirmed the level of cross-priming being decreased in TLR3$^{2/2}$ mice and an expected result was obtained (Fig. S5A,B). Furthermore, in IFNAR$^{2/2}$ mice, OVA-specific CTL induction was slightly reduced compared with that in WT mice, but higher than in TICAM-1$^{2/2}$ mice (Fig. S5C,D). Hence, in vivo cross-presentation induced by polyI:C mostly depends on the TLR3-TICAM-1 pathway followed by transcriptional regulation by IRF-3/7 in any administration route, and is further promoted by type I IFN presumably produced by the stromal cells through the IPS-1 pathway.[26]

IPS-1 induces DC maturation but not cross-priming in vivo. Spleen DC maturation by i.v.-injected polyI:C was tested ex vivo using CD8a⁺ DC and CD8a⁻ DC isolated from WT or KO mice with no tumor as indicated in Figure 5A. The maturation markers

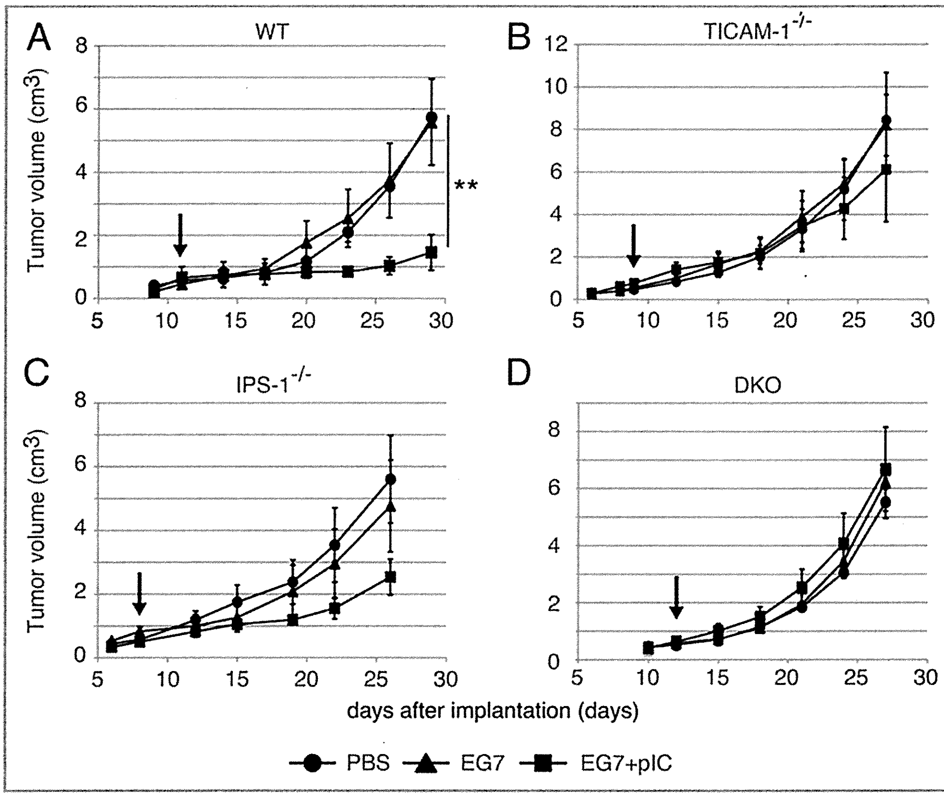

Figure 2. PolyI:C-induced tumor retardation is dependent on the TICAM-1 pathway. Antitumor effect of polyI:C on various KO mice were evaluated by using in vivo mouse tumor implant model. EG7 cells were inoculated to WT (A), TICAM-1$^{2/2}$ (B), IPS-1$^{2/2}$ (C) and DKO mice (D) on day 0. PBS( ), EG7 lysates( ) or EG7 lysates + polyI:C( ) were s.c. administered around the tumor. The adjuvant therapies were started at the time indicated by the arrows and injected twice per week. Each group have 3–4 mice and error bar shows ± SEM. Data are representative of two independent experiments. **: p , 0.01

CD86 and CD40 were upregulated on both CD8a$^+$ and CD8a$^-$ DC from WT mice when they were stimulated with OVA and polyI:C. Treatment of DC with OVA only did not induce upregulation of CD86 and CD40. Although the expression levels of CD86 and CD40 were a little less in CD8a$^+$ and CD8a$^-$ DC from TICAM-1$^{2/2}$ or IPS-1$^{2/2}$ mice than those from WT mice, both CD86 and CD40 were sufficiently upregulated even in the abrogation of either one pathway in polyI:C-injected mice. The CD86 and CD40 shifts were completely abolished in DKO mice (Fig. 5A). Thus, the TICAM-1 pathway participates in both potent co-stimulation and cross-priming, while the IPS-1 pathway mainly participates only in integral co-stimulation in myeloid DC.

We next assessed in vitro proliferation of OT-1 cells. CD8a$^+$ and CD8a$^-$ DC were prepared from PBS, polyI:C, OVA and OVA/polyI:C-treated mice, and mixed in vitro with CFSE-labeled OT-1 cells. WT, TICAM-1$^{2/2}$ and IPS-1$^{2/2}$ mice were used for this study. OT-1 proliferation was observed with CD8a$^+$ DC but not CD8a$^-$ DC when OVA + polyI:C was injected (Fig. 5B). Furthermore, the OT-1 proliferation barely occurred in the mixture containing TICAM-1$^{2/2}$ CD8a$^+$ DC. Thus, OT-1 proliferation is triggered by the TICAM-1 pathway in CD8a$^+$ DC. Again, IPS-1 had almost no effect on OT-1 proliferation with CD8a$^+$ DC in this setting. In the mixture, IFN-c was produced in the supernatants of WT and IPS-1$^{2/2}$ CD8a$^+$ DC but not TICAM-1$^{2/2}$ DC by stimulation with OVA + polyI:C (Fig. 5C). No IFN-c was produced in the supernatants of CD8a$^-$ DC even from WT mice, which results are in parallel with those of OT-1 proliferation. In any case irrespective of tumor-bearing or not, Ag, polyI:C and the TICAM-1 pathway are mandatory for CD8a$^+$ DC to cross-prime and proliferate OVA-specific CD8 T cells.

We checked the TICAM-1- or IPS-1-specific gene expressions related to type I IFN and MHC class I presentation using genechip and qPCR (Fig. S6). PolyI:C-mediated upregulation of Tap1, Tap2 and Tapbp messages diminished in TICAM-1$^{2/2}$ BMDC (Fig. S6A). The levels of these genes were hardly affected in IPS-1$^{2/2}$ BMDC (data not shown). PolyI:C-mediated upregulation was observed with MDA5 (Ifih1) in CD8a$^-$ and CD8a$^+$ DCs (Fig. S6B). Surprisingly, other factors including TLR3, TICAM-1 and MAVS messages were all downregulated in response to polyI:C in CD8a$^+$ DC (Fig. S6B), for the reason as yet unknown.

Effect of TLR3-mediated IFN-inducing pathway on anti-tumor CTL induction. PolyI:C is a dsRNA analog capable of

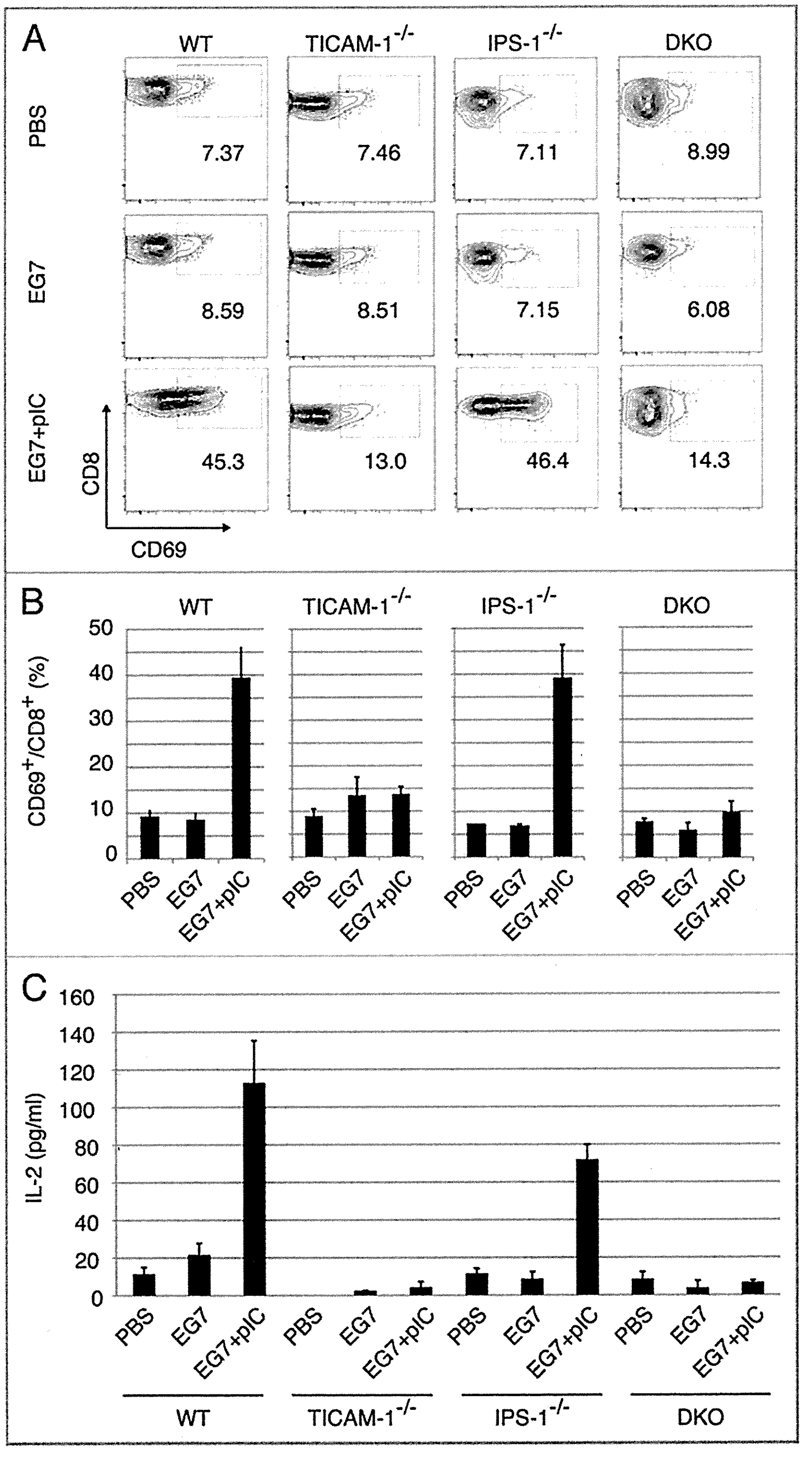

Figure 3. CD8 T cells in the draining LNs are activated through the TICAM-1 pathway by polyI:C. Draining inguinal LNs were harvested from tumor-bearing mice 24 h after the last treatment. LN cells were stained with CD3 , CD8a and CD69, and the cells gated on CD3 $^+$CD8a$^+$ are shown (A). Spleen cells in each group of mice were stained separately, the CD8 levels in gated cells being variably distributed in FACS analyses. The average frequency of activated CD8 T cells defined by CD69 expression is shown (B). Alternatively, LN cells from the indicated mice were cultured for further 3 d in vitro and IL-2 production was measured by CBA assay (C).

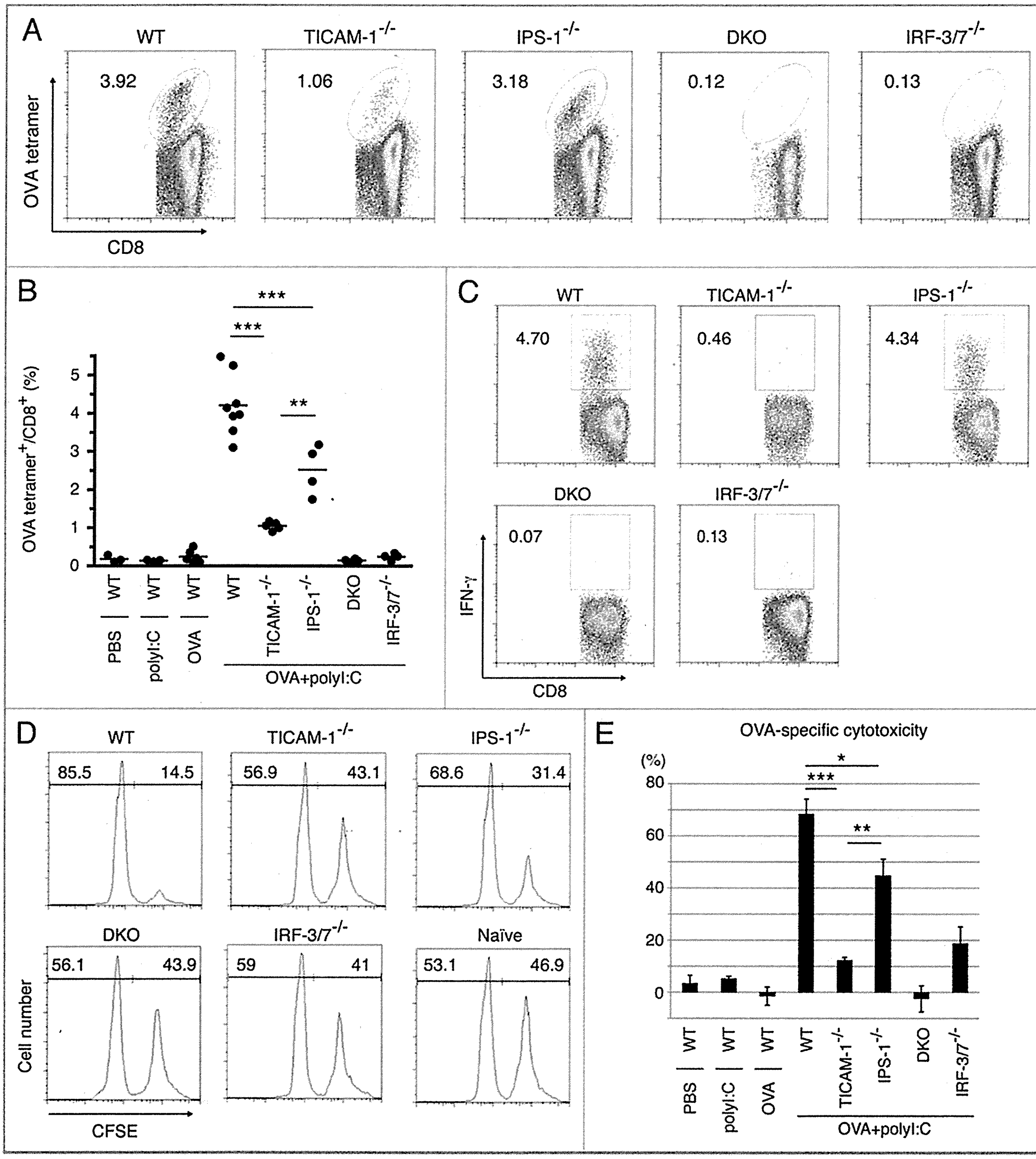

Figure 4. TICAM-1 and IRF-3/7 are essential for polyI:C-induced antigen-specific CTL expansion. WT, TICAM-1$^{2/2}$, IPS-1$^{2/2}$, TICAM-1/IPS-1 DKO and IRF-3/7$^{2/2}$ mice were i.p. administered with the combination of OVA and polyI:C. After 7days, splenocytes were harvested and stained with CD8a and OVA tetramer (A). The average percentages of OVA-specific CTL are shown (B). Alternatively, splenocytes were cultured in vitro in the presence of SL8 for 8 h and IFN-c production was measured by intracellular cytokine staining (C). To assess the killing activity, in vivo CTL assay was performed. The combinations of OVA and polyI:C were administered i.v. to each group of mice and 5 d later, cytotoxicity was measured (D). The data shown are collaborate or representative of at least 3 independent experiments. One-way analysis of variance (ANOVA) with Bonferroni's test was performed to analyze statistical significance. *: p , 0.05, **: p , 0.01, ***: p , 0.001.

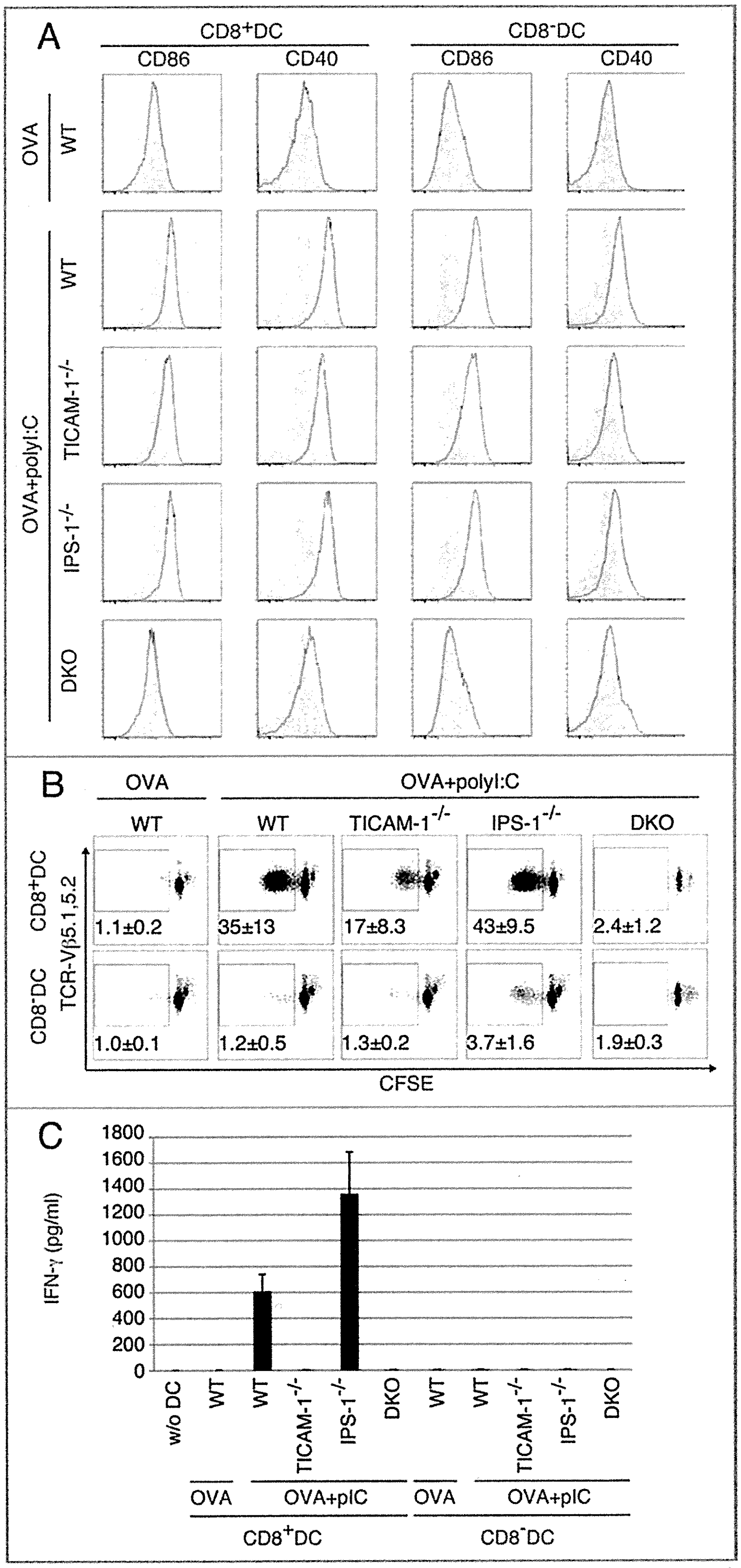

Figure 5. TICAM-1 in CD8a⁺ DC is more important than IPS-1 in polyI:C-induced cross-priming. OVA and polyI:C were administered i.v. and 4 h later, CD8a⁺ and CD8a⁻ DC were isolated from the spleen. CD86 and CD40 expressions were determined by FACS (A). Filled gray and black line show isotype control and target expression, respectively. Alternatively, CD8a⁺ and CD8a⁻ DC were co-cultured with CFSE-labeled RAG2$^{2/2}$/OT-1 T cells for 3 d. The cross-priming activity of each DC subset was determined with sequential dilution of CFSE (B) and IFNc production (C). IFN-c was measured by CBA assay. The data shown are representative of 2 independent experiments. Err bar shows SD.

incorporating into the endosome and cytoplasm by exogenous administration in vitro.[27,28] However, no evidence has been proposed that polyI:C is internalized into the endosome of CD8a⁺ DC where TLR3 is expressed in vivo. Peritoneal (PEC) Mf and bone marrow-derived DC[22] usually phagocytoze polyI:C and deliver them into the endosome. In mouse CD8a⁺ DC direct internalization of polyI:C has remain unproven. Using labeled polyI:C and anti-mouse TLR3 mAb, 11F8,[22] we checked whether the exogenously-added polyI:C encountered with TLR3 in CD8a⁺ DC in vitro. TLR3 (green) was merged with TexasRed-polyI:C 30–120 min after polyI:C stimulation in the culture (Fig. 6A). The quantities of CD8a⁺ and CD8a⁻ DC where FITC-polyI:C was incorporated were determined by FACS analysis (Fig. 6B). Thus, the process by which polyI:C injected reaches the endosomal TLR3 is delineated in the CD8a⁺ DC.

Discussion

PolyI:C is an analog of virus dsRNA, and acts as a ligand for TLR3 and RIG-I/MDA5. PolyI:C has been utilized as an adjuvant for enhancement of antitumor immunity for a long time.[29] However, the mechanistic background of the therapeutic potentials of polyI:C against cancer has been poorly illustrated. It induces antitumor NK activation through DC-NK cell-to-cell interaction when CD8a⁺ DC TLR3 is stimulated in the spleen.[11] Besides myeloid cells, however, some tumor cell lines express TLR3 and dsRNA targeting tumor cells may affect the growth rate of tumors,[30] where the receptor-interacting protein (RIP) pathway is involved downstream of TICAM-1.[31] Here we showed evidence that polyI:C injection facilitates maturation of TLR3-positive CD8a⁺ DC (i.e., APC) to trigger CTL induction against exogenous soluble Ags including EG7 lysate or OVA. The TICAM-1 adaptor for TLR3 and IRF-3/7 are involved in the cross-presentation signal in CD8a⁺ DC, but the molecule/mechanism downstream of

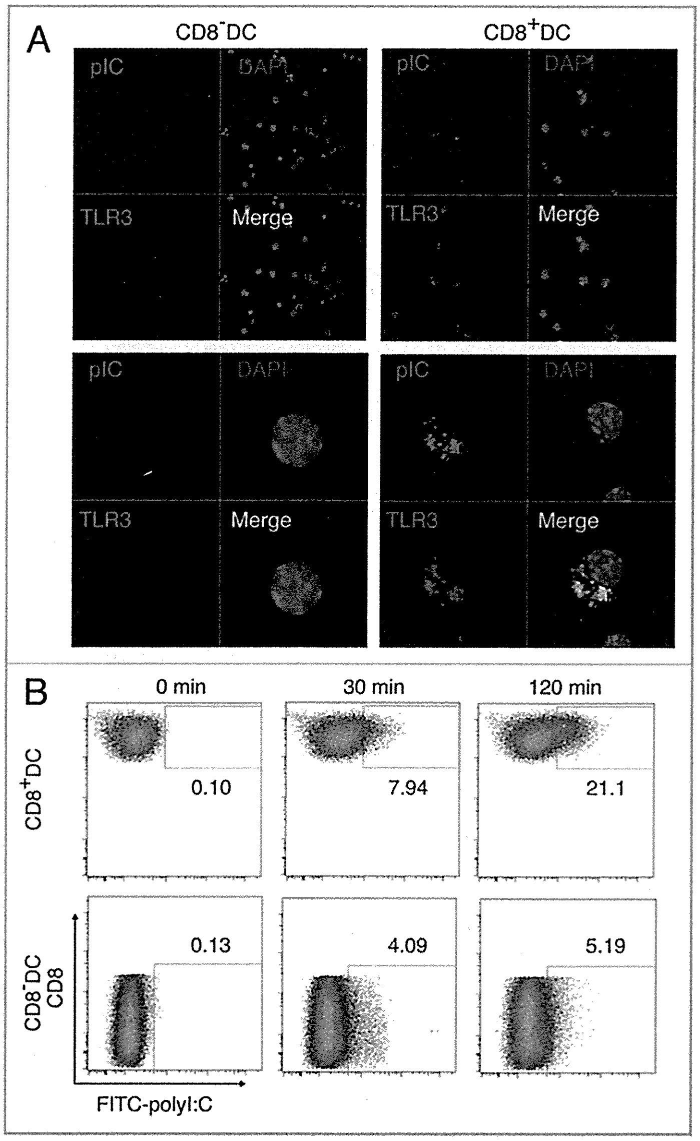

Figure 6. PolyI:C encounters TLR3 in CD8a⁺ DC. CD8a⁺ and CD8a⁻ DC were isolated by FACSAriaII and stimulated with 20 mg/ml TexasRed-polyI:C for 2 h. Then cells were stained with Alexa647-antiTLR3 and subjected to confocal microscopic analysis (A). Alternatively, splenic DC isolated by MACS were incubated with FITC-polyI:C for the time shown in figure and analyzed the degrees of polyI:C uptake by FACS (B). Data shown are the representative of 3 independent experiments.

TICAM-1 that governs cross-presentation remains elusive. Since most of the tumor-associated Ags (TAA) are predicted to be liberated from tumor cells as soluble Ags, the TICAM-1 pathway in CD8a⁺ DC would be crucial for driving of tumor-specific CTL around the tumor microenvironment. In any route of polyI:C injection, this is true as shown first in this study. Although TICAM-1 is an adaptor of other cytoplasmic sensors, DDX1, DDX21 and DHX36,[32] the antitumor CTL responses are merely relied on TLR3 of CD8a⁺DC in this system. Taken together with previous reports,[11,12] TICAM-1 signaling triggers not only NK activation but also CTL induction.

TLR3 and MDA5 are main sensors for dsRNA and differentially distributed in myeloid cells.[33,34] TLR3 is limitedly expressed in myeloid, epithelial and neuronal cells,[33] whereas MDA5 is ubiquitously expressed including non-myeloid stromal cells.[33] Several reports suggested that i.v. injection of polyI:C predominantly stimulate the stromal cells which express IFNAR,[26] thereby robust type I IFN are liberated from these cells to be a systemic response including cytokinemia and endotoxin-like shock.[35,36] Both TLR3 and MDA5 link to the IRF-3/7-activating kinases leading to the production of IFNa/ .[37,38] Once IFNa/ are released, IFNAR senses it to amplify the type I IFN production,[39] and reportedly this amplification pathway involves cross-priming of CD8 T cells in viral infection.[18] Tumor progression or metastasis can be suppressed through the IFNAR pathway.[40] These scenarios may be right depending on the conditions employed. Our message is related to what signal pathway is fundamentally required for induction of antitumor CTL in DC. The CTL response is almost completely abrogated in TICAM-1$^{2/2}$ and IRF-3/7$^{2/2}$ mice, but largely remains in IPS-1$^{2/2}$ and IFNAR$^{2/2}$ mice when Ag and polyI:C are extrinsically administered. The results are reproducible in some other tumor-implant models (data not shown), and even in IFNAR$^{2/2}$ mice, TICAM-1-specific genes are upregulated to confer tumor cytotoxicity (Fig. S6, Azuma et al., unpublished data). In addition, the upregulation of these genes is independent of IPS-1 knockout in DC. Our results infer that the primary sensing of dsRNA in CD8a⁺ DC is competent to induce cross-presentation, which minimally involves the IPS-1 or IFNAR amplification pathway, at least at a low dose of polyI:C. Yet, subsequent induction of type I IFN via the IFNAR may further amplify the cross-priming.[18,41] Further studies are needed as to which of the TICAM-1-inducible genes link to the cross-presentation in CD8a⁺ DC.

The main focus of this study was to identify the pathway for transversion of immature DC to the CTL-driving phenotype by co-administration of polyI:C with soluble Ag. The IPS-1 pathway, although barely participates in antitumor CTL driving, can upregulate CD40/CD86 co-stimulators on the membranes of splenic CD8a⁺ and CD8a⁻ DC in response to polyI:C, suggesting that MDA5 does function in the cytoplasm of splenic CD8a⁺ and CD8a⁻ DC to sense polyI:C. However, effective CTL induction happens only in CD8a⁺ DC when stimulated with polyI:C. CD8a⁺ DC express TLR3 but CD8a⁻ DC do not, and CD8a⁺ DC with no TLR3 fail to induce CTL, suggesting that integral co-stimulation by MDA5/IPS-1 is insufficient for DC to induce cross-priming of CD8 T cells: antitumor CTL are not induced until the TICAM-1 signal is provided in DC. At least, sole effect of the IPS-1 pathway and upregulation of co-stimulators on CD8a⁺ DC is limited for cross-priming and induction of antitumor CTL, which result partly reflects those in a previous report where IPS-1 and TICAM-1 harbor a similar potential for CD8 T cell proliferation when polyI:C (Alum-containing) is employed as an adjuvant for CD8a$^+$ DC to test proliferation of anti-OVA CTL.[21]

A question is why TICAM-1 is dominant to IPS-1 for response to exogenously-added polyI:C in CD8a$^+$ DC. The answer is rooted in the difference of functional behavior between BMDC and CD8a$^+$ DC. TLR3 levels are variable depending upon subsets of DC,[22] which affects DC subset-specific induction of cellular immune response. The high TLR3 expression (partly surface-expressed) is situated in CD8a$^+$ DC before polyI:C stimulation, which is distinct from the properties of F4/80$^+$ Mf and presumably BMDC of low TLR3 expression. The polyI:C-uptake machinery[15] appears to efficiently work in concert with the TLR3/TICAM-1 pathway in CD8a$^+$ DC and this tendency is diminished when CD8a$^+$ DC are pretreated with Alum + polyI:C.[21] Furthermore, there are functional discrepancies between CD8a$^+$ splenic DC and GM-CSF-induced BMDC, which appears to reflect the difference of their TLR3 levels.[22] These results on CD8a$^+$ DC encourage us to develop dsRNA adjuvant immunotherapy supporting TAA soluble vaccines for cancer applicable to humans, which possess the counterpart of CD8a$^+$ DC.

There are two modes of dsRNA-mediated DC maturation, intrinsic and extrinsic modes that are governed by the IPS-1 and TICAM-1 pathways, respectively.[9,34] It is important to elucidate the in vivo qualitative difference in the two pathways in tumor-loading mice. TLR3$^+$ DC/Mf are responsible for CTL driving via an extrinsic route in viral infection.[34] Previous data suggested that dsRNA in infectious cell debris, rather than viral dsRNA produced in the cytoplasm of Ag-presenting cells or autophagosome formation, contribute to fine tuning of DC maturation through extrinsic dsRNA recognition.[16] It is reported that dsRNA-containing debris are generated secondary to infection-mediated cell death,[41] and DC phagocytose by-stander dead cells. Likewise, soluble tumor Ags released from tumor cells usually are extrinsically taken up by APC in patients with cancer.[42] If CTL are successfully induced in therapeutic biotherapy targeted against cancer cells, this extrinsic TICAM-1 pathway must be involved in the therapeutic process.

Cross-presentation occurs in a TAP-dependent[43] and -independent fashions.[44,45] The peptides are transported by TAP into the endoplasmic reticulum (ER) and loaded onto MHC class I for presentation at the cell surface. ER and phagosome might fuse each other for accelerating cross-presentation.[46] Another possibility is that cross-presentation occurs in early endosomes where TLR3 resides. This early endosome cross-presentation does not always depend on TAP[42-44] but requires TLR stimulation.[34] TLR4/MyD88 pathway is involved in the TAP-dependent early endosome model,[43] where recruitment of TAP to the early endosomes is an essential step for the cross-presentation of soluble Ag. These models together with our genechip analysis of polyI:C-stimulated BMDC suggested that some ER-associated proteins are upregulated in BMDC by polyI:C-TICAM-1 pathway. The results infer that the TLR3/TICAM-1 rather than the TLR4/MyD88 pathway more crucially participates in cross-presentation in response to dsRNA or viral stimuli and facilitates raising CTL antitumor immunity in APC.

Although multiple RNA sensors couple with TICAM-1 and signal to activate the type I IFN-inducing pathway,[25] at least TLR3 in the CD8a$^+$ DC are critical in CTL driving. CD8a$^+$ DC are a high TLR3 expresser, while BMDC express TLR3 with only low levels.[22] CD8a$^-$ DC do not express it.[22] The Ag presentation and TLR3 levels in CD8a$^+$ DC appear reciprocally correlated with the phagocytosing ability of DC. Although the TLR3 mRNA level is downregulated secondary to polyI:C response after maturation, this may not be related to the CD8a$^+$ DC functions. Yet, polyI:C might interact with other cytoplasmic sensors for DC maturation,[32,47]

The route of administration and delivery methods may be important for culminate the polyI:C adjuvant function. The toxic problem has not overcome in the adjuvant therapy using polyI:C[35,36] and this is a critical matter for clinical introduction of dsRNA reagents to immunotherapy. The most problematic is the life-threatening shock induced by polyI:C. Recent advance of polyI:C study suggests that PEI-jet helps efficient uptake of polyI:C into peritoneal macrophages.[48] LC (poly-L-lysine and methylcellulose) has been used as a preservative to reduce the toxic effect of polyI:C.[49] Nanotechnological delivery of polyI:C results in efficient tumor regression.[50] There are many subsets of DC that can be defined by surface markers, and selecting an appropriate administration route can target a specific DC subset. The route for s.c. administration usually mature dermal/epidermal DC or Langerhans cells.[51,52] Some DC subsets with unique properties specialized to CTL induction would work in association with the route of polyI:C administration. Attempting to develop more harmless and efficient dsRNA derivatives will benefit for establishing human adjuvant immunotherapy for cancer.

Materials and Methods

Mice. TICAM-1$^{2/2}$ and IPS-1$^{2/2}$ mice were made in our laboratory and backcrossed more than 8 times to adapt C57BL/6 background.[12] IRF-3/7$^{2/2}$ and IFNAR$^{2/2}$ mice were kindly provided by T. Taniguchi (University of Tokyo, Tokyo, Japan). TLR3$^{2/2}$ mice were kindly provided by S. Akira (Osaka University, Osaka, Japan). Rag2$^{2/2}$ and OT-1 mice were kindly provided from Drs. N. Ishii (Tohoku Univ. Sendai, Japan). Rag2$^{2/2}$/OT-1 mice were bred in our laboratory. All mice were maintained under specific pathogen-free conditions in the animal facility of the Hokkaido University Graduate School of Medicine. Animal experiments were performed according to the guidelines set by the animal safety center, Hokkaido University, Japan.

Cells. EG7 and C1498 cells were purchased from ATCC and cultured in RPMI1640/10% FCS/55 mM 2-ME/1 mM sodium pyruvate and RPMI1640/10% FCS/25 ng/ml 2-ME, respectively. Mouse splenocytes, OT-1 T cell, CD8a$^+$ DC and CD8a$^-$ DC were harvested from the spleen and cultured in RPMI1640/10% FCS/55mM 2-ME/10mM HEPES.[41] B16D8 cells were cultured in RPMI/10% FCS as described previously.[12]

Reagents and antibodies. Ovalbumin (OVA) and polyI:C (polyI:C) were purchased from SIGMA and Amersham

Biosciences, respectively. $OVA_{257-264}$ peptide (SIINFEKL: SL8) and OVA ($H2K^b$-SL8) Tetramer were from MBL. Following Abs were purchased: anti-CD3 (145-2C11), anti-CD8 (53-6.7), anti-CD11c (N418), anti-CD16/32 (93), anti-CD69 (H1.2F3) and anti-IFNC(XMG1.2) Abs from BioLegend, anti-B220 (RA3-6B2), anti-CD4 (L3T4), anti-CD40 (1C10), anti-CD86 (GL1), and anti-MHC I-SL8 (25-D1.16) Abs from eBiosciences, anti-TCR-V 5.1/5.2 Ab and ViaProbe from BD Biosciences. The Rat anti-mouse TLR3 mAb (11F8) was kindly provided by David M. Segal (National Institute of Health, Bethesda, MD). To rule out LPS contamination, we treated OVA or other reagents with 200 mg/ml of Polymixin B for 30 min at 37°C before use. Texas Red- or FITC-labeled poly(I:C) was prepared using the 5' EndTag™ Nucleic Acid Labeling System (Vector Laboratories) according to the manufacturers instructions.

Tumor challenge and poly I:C therapy. Mice were shaved at the back and s.c. injected with 200 ml of 2 10^6 syngenic EG7 cells in PBS. Tumor volumes were measured at regular intervals by using a caliper. Tumor volume was calculated by using the formula: Tumor volume (cm^3) = (long diameter) (short diameter)^2 0.4. A volume of 50 ml of a mixture consisting of the lysate of 2 10^5 EG7 cells with or without 50 mg of poly I:C (polyI:C) was s.c. injected around the tumor. We added no other emulsified reagent for immunization since we want to role out the conditional effect of the Ag/polyI:C. The treatments were started when the average of tumor volumes reached at 0.4–0.8 cm^3 and performed twice per week. EG7 lysate were prepared by three times freeze/thaw cycles (-140°C/37°C) in PBS, with removal of cell debris by centrifugation at 6,000 g for 10 min.[53] To deplete CD8 T cells, mice were i.p. injected with hybridoma ascites of anti-CD8 mAb. The dose of antibody and the treatment regimens were determined in preliminary studies by using the same lots of antibody used for the experiments. Depletion of the desired cell populations by this treatment was confirmed by FACS for the entire duration of the study.

Evaluation of T cell activity in tumor-bearing mice. Draining inguinal LN cells were harvested from tumor-bearing mice after 24 hrs from the last polyI:C treatment. The activity of T cells was evaluated by CD69 expression and IL-2/IFNC production. These cells were stained with FITC-CD8a, PE-CD69, PerCP/Cy5.5-7AAD and APC-CD3 . To check cytokine production, LN cells were cultured for 3 d in vitro in the presence or absence of EG7 lysates and IL-2 and IFNC productions were determined by Cytokine Beads Array (CBA) assay (BD). To assess the cytotoxic activity of CTL, standard ^{51}Cr release assay was performed. For CTL expansion, 2.5 10^6 LN cells were co-cultured with 1.25 10^5 mitomycin C-treated EG7 cells in the presence of 10 U/ml IL-2 for 5 d. Then, LN cells were incubated with ^{51}Cr-labeled EG7 or C1498 cells for 4 h and determined cytotoxic activity. The cell-specific cytotoxicity was calculated with subtracting the cytotoxity for C1498 from for EG7 cells.

Antigen-specific T cell expansion in vivo. Mice were i.p. immunized with 1 mg of OVA and 150 mg of poly I:C. After 7 d, spleens were homogenized and stained with FITC-CD8a and PE-OVA Tetramer for detecting OVA-specific CD8 T cell populations. For intracellular cytokine detection, splenocytes were cultured with or without 100 nM OVA peptide (SIINFEKL; SL8) for 8 h and 10 mg/ml of Brefeldin A (Sigma-Aldrich) was added to the culture in the last 4 h. Then cells were stained with PE-anti-CD8a and fixed/permeabilized with Cytofix/Cytoperm (BD Biosciences) according to manufacturer's instruction. Then, fixed/permeabilized cells were further stained with APC-anti-IFNC. Stained cells were analyzed with FACSCalibur (BD Biosciences) and FlowJo software (Tree Star).

In vivo CTL assay. The in vivo CTL assay was performed as described.[54] In brief, WT, TICAM-1$^{2/2}$, MAVS$^{2/2}$ and IRF-3/7$^{2/2}$ mice were i.v. administered with PBS, 10 mg of OVA or OVA with 50 mg of polyI:C. After 5 d, 2 10^7 target cells (see below) were i.v. injected to other irrelevant mice and 8 h later, the OVA-specific cytotoxicity was measured by FACSCalibur. Target cells were 1:1 mixture of 2 mM SL8-pulsed, 5 mM CFSE-labeled splenocytes and SL8-unpulesed, 0.5 mM CFSE-labeled splenocytes. OVA-specific cytotoxicity was calculated with a formula: [1-(Primed ($CFSE^{high}$(%)/$CFSE^{low}$(%))/Unprimed ($CFSE^{high}$(%)/$CFSE^{low}$(%))] 100.

DC preparation. DCs were prepared from spleens of mice, as described previously.[55] In brief, collagenase-digested spleen cells were treated with ACK buffer and then washed with PBS twice. Then splenocytes were positively isolated with anti-CD11c MicroBeads. CD11c$^+$ cells were acquired routinely about $ 80% purity. Further, to highly purify CD8a$^+$ and CD8a$^-$ DCs, spleen DC were stained with FITC-CD8a, PE-B220, PE/Cy7-CD11c and PerCP5.5-7AAD. CD8a$^+$ or CD8a$^-$ CD11c$^+$B220$^-$ DCs were purified on FACSAriaII (BD). The purity of the cells was $ 98%.

OT-1 proliferation assay. Ten mg of OVA with or without 50 mg of polyI:C were i.v. injected to WT, TICAM-1$^{2/2}$, IPS-1$^{2/2}$ and DKO mice. After 4 h, CD8a$^+$ or CD8a$^-$ DC were purified from the spleen. 2.5 10^4 CD8a$^+$ or CD8a$^-$ DC were co-cultured with 5 10^4 1 mM CFSE-labeled Rag2$^{2/2}$/OT-1 T cells for 3 d in 96-well round bottom plate. These cells were stained with PE-anti-TCR-V 5.1,5.2 and APC-anti-CD3 and T cell proliferation was analyzed by CFSE dilution using FACSCalibur. Additionally, IFNC in the culture supernatant was measured by CBA assay.

Statistical analysis. P-values were calculated with one-way analysis of variance (ANOVA) with Bonferroni's test. Error bars represent the SD or SEM between samples.

Disclosure of Potenial Conflicts of Interest

No potential conflicts of interest were disclosed.

Acknowledgment

We are grateful to Drs. T. Taniguchi (Univ. Tokyo, Tokyo), N. Ishii (Tohoku Univ., Sendai) and D. M. Segel (NCI, Bethesda) for providing us with IRF-3/7$^{2/2}$ mice, OT-1 mice and anti-monse TLR3 mAb, respectively. Invaluable discussions about the peptide vaccine therapy with Dr. N. Satoh (Sapporo Medical Univ., Sapporo) are gratefully acknowledged. We thank Drs. H. Takaki, J. Kasamatsu, H. H.Aly, and H. Shime in our lab for their critical comments on this study.

This work was supported in part by Grants-in-Aid from the Ministry of Education, Science, and Culture (Specified Project for Advanced Research, MEXT) and the Ministry of Health, Labor, and Welfare of Japan, and by the Takeda and the Waxmann Foundations. Financial supports by a MEXT Grant-in-Project "The Carcinogenic Spiral" is gratefully acknowledged.

References

1. Iwasaki A, Medzhitov R. Regulation of adaptive immunity by the innate immune system. Science 2010; 327:291-5; PMID:20075244; http://dx.doi.org/10.1126/science.1183021
2. Seya T, Shime H, Ebihara T, Oshiumi H, Matsumoto M. Pattern recognition receptors of innate immunity and their application to tumor immunotherapy. Cancer Sci 2010; 101:313-20; PMID:20059475; http://dx.doi.org/10.1111/j.1349-7006.2009.01442.x
3. Akira S. Toll-like receptor signaling. J Biol Chem 2003; 278:38105-8; PMID:12893815; http://dx.doi.org/10.1074/jbc.R300028200
4. Kawai T, Akira S. The roles of TLRs, RLRs and NLRs in pathogen recognition. Int Immunol 2009; 21:317-37; PMID:19246554; http://dx.doi.org/10.1093/intimm/dxp017
5. Longman RS, Braun D, Pellegrini S, Rice CM, Darnell RB, Albert ML. Dendritic-cell maturation alters intracellular signaling networks, enabling differential effects of IFN-alpha/beta on antigen cross-presentation. Blood 2007; 109:1113-22; PMID:17018853; http://dx.doi.org/10.1182/blood-2006-05-023465
6. Shinohara ML, Kim JH, Garcia VA, Cantor H. Engagement of the type I interferon receptor on dendritic cells inhibits T helper 17 cell development: role of intracellular osteopontin. Immunity 2008; 29:68-78; PMID:18619869; http://dx.doi.org/10.1016/j.immuni.2008.05.008
7. Diebold SS. Recognition of viral single-stranded RNA by Toll-like receptors. Adv Drug Deliv Rev 2008; 60:813-23; PMID:18241955; http://dx.doi.org/10.1016/j.addr.2007.11.004
8. Matsumoto M, Oshiumi H, Seya T. Antiviral responses induced by the TLR3 pathway. Rev Med Virol 2011. Epub ahead of print. PMID:21312311; http://dx.doi.org/10.1002/rmv.680
9. Yoneyama M, Fujita T. RIG-I family RNA helicases: cytoplasmic sensor for antiviral innate immunity. Cytokine Growth Factor Rev 2007; 18:545-51; PMID:17683970; http://dx.doi.org/10.1016/j.cytogfr.2007.06.023
10. Seya T, Matsumoto M. The extrinsic RNA-sensing pathway for adjuvant immunotherapy of cancer. Cancer Immunol Immunother 2009; 58:1175-84; PMID:19184005; http://dx.doi.org/10.1007/s00262-008-0652-9
11. Akazawa T, Ebihara T, Okuno M, Okuda Y, Shingai M, Tsujimura K, et al. Antitumor NK activation induced by the Toll-like receptor 3-TICAM-1 (TRIF) pathway in myeloid dendritic cells. Proc Natl Acad Sci U S A 2007; 104:252-7; PMID:17190817; http://dx.doi.org/10.1073/pnas.0605978104
12. Ebihara T, Azuma M, Oshiumi H, Kasamatsu J, Iwabuchi K, Matsumoto K, et al. Identification of a polyI:C-inducible membrane protein that participates in dendritic cell-mediated natural killer cell activation. J Exp Med 2010; 207:2675-87; PMID:21059856; http://dx.doi.org/10.1084/jem.20091573
13. Perrot I, Deauvieau F, Massacrier C, Hughes N, Garrone P, Durand I, et al. TLR3 and Rig-like receptor on myeloid dendritic cells and Rig-like receptor on human NK cells are both mandatory for production of IFN-gamma in response to double-stranded RNA. J Immunol 2010; 185:2080-8; PMID:20639488; http://dx.doi.org/10.4049/jimmunol.1000532
14. Bevan MJ. Cross-priming for a secondary cytotoxic response to minor H antigens with H-2 congenic cells which do not cross-react in the cytotoxic assay. J Exp Med 1976; 143:1283-8; PMID:1083422; http://dx.doi.org/10.1084/jem.143.5.1283
15. Datta SK, Redecke V, Prilliman KR, Takabayashi K, Corr M, Tallant T, et al. A subset of Toll-like receptor ligands induces cross-presentation by bone marrow-derived dendritic cells. J Immunol 2003; 170:4102-10; PMID:12682240
16. Schulz O, Diebold SS, Chen M, Näslund TI, Nolte MA, Alexopoulou L, et al. Toll-like receptor 3 promotes cross-priming to virus-infected cells. Nature 2005; 433:887-92; PMID:15711573; http://dx.doi.org/10.1038/nature03326
17. Kono H, Rock KL. How dying cells alert the immune system to danger. Nat Rev Immunol 2008; 8:279-89; PMID:18340345; http://dx.doi.org/10.1038/nri2215
18. Le Bon A, Etchart N, Rossmann C, Ashton M, Hou S, Gewert D, et al. Cross-priming of CD8+ T cells stimulated by virus-induced type I interferon. Nat Immunol 2003; 4:1009-15; PMID:14502286; http://dx.doi.org/10.1038/ni978
19. Bennett SR, Carbone FR, Karamalis F, Miller JF, Heath WR. Induction of a CD8+ cytotoxic T lymphocyte response by cross-priming requires cognate CD4+ T cell help. J Exp Med 1997; 186:65-70; PMID:9206998; http://dx.doi.org/10.1084/jem.186.1.65
20. Shimizu K, Kurosawa Y, Taniguchi M, Steinman RM, Fujii S. Cross-presentation of glycolipid from tumor cells loaded with alpha-galactosylceramide leads to potent and long-lived T cell mediated immunity via dendritic cells. J Exp Med 2007; 204:2641-53; PMID:17923500; http://dx.doi.org/10.1084/jem.20070458
21. Kumar H, Koyama S, Ishii KJ, Kawai T, Akira S. Cutting edge: cooperation of IPS-1- and TRIF-dependent pathways in poly IC-enhanced antibody production and cytotoxic T cell responses. J Immunol 2008; 180:683-7; PMID:18178804
22. Jelinek I, Leonard JN, Price GE, Brown KN, Meyer-Manlapat A, Goldsmith PK, et al. TLR3-specific double-stranded RNA oligonucleotide adjuvants induce dendritic cell cross-presentation, CTL responses, and antiviral protection. J Immunol 2011; 186:2422-9; PMID:21242525; http://dx.doi.org/10.4049/jimmunol.1002845
23. Wang Y, Cella M, Gilfillan S, Colonna M. Cutting edge: polyinosinic:polycytidylic acid boosts the generation of memory CD8 T cells through melanoma differentiation-associated protein 5 expressed in stromal cells. J Immunol 2010; 184:2751-5; PMID:20164430; http://dx.doi.org/10.4049/jimmunol.0903201
24. Carbone FR, Bevan MJ. Induction of ovalbumin-specific cytotoxic T cells by in vivo peptide immunization. J Exp Med 1989; 169:603-12; PMID:2784478; http://dx.doi.org/10.1084/jem.169.3.603
25. Asano J, Tada H, Onai N, Sato T, Horie Y, Fujimoto Y, et al. Nucleotide oligomerization binding domain-like receptor signaling enhances dendritic cell-mediated cross-priming in vivo. J Immunol 2010; 184:736-45; PMID:20008287; http://dx.doi.org/10.4049/jimmunol.0900726
26. McCartney S, Vermi W, Gilfillan S, Cella M, Murphy TL, Schreiber RD, et al. Distinct and complementary functions of MDA5 and TLR3 in poly(I:C)-mediated activation of mouse NK cells. J Exp Med 2009; 206:2967-76; PMID:19995959; http://dx.doi.org/10.1084/jem.20091181
27. Watanabe A, Tatematsu M, Saeki K, Shibata S, Shime H, Yoshimura A, et al. Raftlin is involved in the nucleocapture complex to induce poly(I:C)-mediated TLR3 activation. J Biol Chem 2011; 286:10702-11; PMID:21266579; http://dx.doi.org/10.1074/jbc.M110.185793
28. Itoh K, Watanabe A, Funami K, Seya T, Matsumoto M. The clathrin-mediated endocytic pathway participates in dsRNA-induced IFN-beta production. J Immunol 2008; 181:5522-9; PMID:18832709
29. Talmadge JE, Adams J, Phillips H, Collins M, Lenz B, Schneider M, et al. Immunomodulatory effects in mice of polyinosinic-polycytidylic acid complexed with poly-L-lysine and carboxymethylcellulose. Cancer Res 1985; 45:1058-65; PMID:3155990
30. Conforti R, Ma Y, Morel Y, Paturel C, Terme M, Viaud S, et al. Opposing effects of toll-like receptor (TLR3) signaling in tumors can be therapeutically uncoupled to optimize the anticancer efficacy of TLR3 ligands. Cancer Res 2010; 70:490-500; PMID:20068181; http://dx.doi.org/10.1158/0008-5472.CAN-09-1890
31. Kaiser WJ, Offermann MK. Apoptosis induced by the toll-like receptor adaptor TRIF is dependent on its receptor interacting protein homotypic interaction motif. J Immunol 2005; 174:4942-52; PMID:15814722
32. Zhang Z, Kim T, Bao M, Facchinetti V, Jung SY, Ghaffari AA, et al. DDX1, DDX21, and DHX36 helicases form a complex with the adaptor molecule TRIF to sense dsRNA in dendritic cells. Immunity 2011; 34:866-78; PMID:21703541; http://dx.doi.org/10.1016/j.immuni.2011.03.027
33. Gitlin L, Barchet W, Gilfillan S, Cella M, Beutler B, Flavell RA, et al. Essential role of mda-5 in type I IFN responses to polyriboinosinic:polyribocytidylic acid and encephalomyocarditis picornavirus. Proc Natl Acad Sci U S A 2006; 103:8459-64; PMID:16714379; http://dx.doi.org/10.1073/pnas.0603082103
34. Matsumoto M, Seya T. TLR3: interferon induction by double-stranded RNA including poly(I:C). Adv Drug Deliv Rev 2008; 60:805-12; PMID:18262679; http://dx.doi.org/10.1016/j.addr.2007.11.005
35. Absher M, Stinebring WR. Toxic properties of a synthetic double-stranded RNA. Endotoxin-like properties of poly I. poly C, an interferon stimulator. Nature 1969; 223:715-7; PMID:5805520; http://dx.doi.org/10.1038/223715a0
36. Berry LJ, Smythe DS, Colwell LS, Schoengold RJ, Actor P. Comparison of the effects of a synthetic polyribonucleotide with the effects of endotoxin on selected host responses. Infect Immun 1971; 3:444-8; PMID:16557994
37. Sasai M, Shingai M, Funami K, Yoneyama M, Fujita T, Matsumoto M, et al. NAK-associated protein 1 participates in both the TLR3 and the cytoplasmic pathways in type I IFN induction. J Immunol 2006; 177:8676-83; PMID:17142768
38. Ishikawa H, Barber GN. STING is an endoplasmic reticulum adaptor that facilitates innate immune signalling. Nature 2008; 455:674-8; PMID:18724357; http://dx.doi.org/10.1038/nature07317
39. Taniguchi T, Takaoka A. A weak signal for strong responses: interferon-alpha/beta revisited. Nat Rev Mol Cell Biol 2001; 2:378-86; PMID:11331912; http://dx.doi.org/10.1038/35073080
40. Ogasawara S, Yano H, Momosaki S, Akiba J, Nishida N, Kojiro S, et al. Growth inhibitory effects of IFN-beta on human liver cancer cells in vitro and in vivo. J Interferon Cytokine Res 2007; 27:507-16; PMID:17572015; http://dx.doi.org/10.1089/jir.2007.0183

41. Ebihara T, Shingai M, Matsumoto M, Wakita T, Seya T. Hepatitis C virus-infected hepatocytes extrinsically modulate dendritic cell maturation to activate T cells and natural killer cells. Hepatology 2008; 48:48-58; PMID:18537195; http://dx.doi.org/10.1002/hep.22337
42. Chaput N, Conforti R, Viaud S, Spatz A, Zitvogel L. The Janus face of dendritic cells in cancer. Oncogene 2008; 27:5920-31; PMID:18836473; http://dx.doi.org/10.1038/onc.2008.270
43. Burgdorf S, Schölz C, Kautz A, Tampé R, Kurts C. Spatial and mechanistic separation of cross-presentation and endogenous antigen presentation. Nat Immunol 2008; 9:558-66; PMID:18376402; http://dx.doi.org/10.1038/ni.1601
44. Shen L, Sigal LJ, Boes M, Rock KL. Important role of cathepsin S in generating peptides for TAP-independent MHC class I crosspresentation in vivo. Immunity 2004; 21:155-65; PMID:15308097; http://dx.doi.org/10.1016/j.immuni.2004.07.004
45. Kurotaki T, Tamura Y, Ueda G, Oura J, Kutomi G, Hirohashi Y, et al. Efficient cross-presentation by heat shock protein 90-peptide complex-loaded dendritic cells via an endosomal pathway. J Immunol 2007; 179:1803-13; PMID:17641047
46. Gagnon E, Duclos S, Rondeau C, Chevet E, Cameron PH, Steele-Mortimer O, et al. Endoplasmic reticulum-mediated phagocytosis is a mechanism of entry into macrophages. Cell 2002; 110:119-31; PMID:12151002; http://dx.doi.org/10.1016/S0092-8674(02)00797-3
47. Samuel CE. Antiviral actions of interferons. Clin Microbiol Rev 2001; 14:778-809; PMID:11585785; http://dx.doi.org/10.1128/CMR.14.4.778-809.2001
48. Wu CY, Yang HY, Monie A, Ma B, Tsai HH, Wu TC, et al. Intraperitoneal administration of poly(I:C) with polyethylenimine leads to significant antitumor immunity against murine ovarian tumors. Cancer Immunol Immunother 2011; 60:1085-96; PMID:21526359; http://dx.doi.org/10.1007/s00262-011-1013-7
49. Longhi MP, Trumpfheller C, Idoyaga J, Caskey M, Matos I, Kluger C, et al. Dendritic cells require a systemic type I interferon response to mature and induce CD4+ Th1 immunity with poly IC as adjuvant. J Exp Med 2009; 206:1589-602; PMID:19564349; http://dx.doi.org/10.1084/jem.20090247
50. Kitano S, Kageyama S, Nagata Y, Miyahara Y, Hiasa A, Naota H, et al. HER2-specific T-cell immune responses in patients vaccinated with truncated HER2 protein complexed with nanogels of cholesteryl pullulan. Clin Cancer Res 2006; 12:7397-405; PMID:17189412; http://dx.doi.org/10.1158/1078-0432.CCR-06-1546
51. Kushwah R, Hu J. Complexity of dendritic cell subsets and their function in the host immune system. Immunology 2011; 133:409-19; PMID:21627652; http://dx.doi.org/10.1111/j.1365-2567.2011.03457.x
52. Asano K, Nabeyama A, Miyake Y, Qiu CH, Kurita A, Tomura M, et al. CD169-positive macrophages dominate antitumor immunity by crosspresenting dead cell-associated antigens. Immunity 2011; 34:85-95; PMID:21194983; http://dx.doi.org/10.1016/j.immuni.2010.12.011
53. Galea-Lauri J, Wells JW, Darling D, Harrison P, Farzaneh F. Strategies for antigen choice and priming of dendritic cells influence the polarization and efficacy of antitumor T-cell responses in dendritic cell-based cancer vaccination. Cancer Immunol Immunother 2004; 53:963-77; PMID:15146294; http://dx.doi.org/10.1007/s00262-004-0542-8
54. Durand V, Wong SY, Tough DF, Le Bon A. Shaping of adaptive immune responses to soluble proteins by TLR agonists: a role for IFN-a/ . Immunol Cell Biol 2004; 82:596-602; PMID:15550117; http://dx.doi.org/10.1111/j.0818-9641.2004.01285.x
55. Yamazaki S, Okada K, Maruyama A, Matsumoto M, Yagita H, Seya T. TLR2-dependent induction of IL-10 and Foxp3+ CD25+ CD4+ regulatory T cells prevents effective anti-tumor immunity induced by Pam2 lipopeptides in vivo. PLoS One 2011; 6:e18833; PMID:21533081; http://dx.doi.org/10.1371/journal.pone.0018833

Toll-like receptor 3 signaling converts tumor-supporting myeloid cells to tumoricidal effectors

Hiroaki Shime[a], Misako Matsumoto[a], Hiroyuki Oshiumi[a], Shinya Tanaka[b], Akio Nakane[c], Yoichiro Iwakura[d], Hideaki Tahara[e], Norimitsu Inoue[f], and Tsukasa Seya[a,1]

[a]Department of Microbiology and Immunology, and [b]Department of Cancer Pathology, Graduate School of Medicine, Hokkaido University, Kita-ku, Sapporo 060-8638, Japan; [c]Department of Microbiology and Immunology, Graduate School of Medicine, Hirosaki University, Zaifu-cho, Hirosaki 036-8562, Japan; [d]Laboratory of Molecular Pathogenesis, Center for Experimental Medicine and Systems Biology, and [e]Department of Surgery and Bioengineering, Advanced Clinical Research Center, Institute of Medical Science, University of Tokyo, Shirokanedai, Minato-ku, Tokyo 108-8639, Japan; and [f]Department of Molecular Genetics, Osaka Medical Center for Cancer, Nakamichi, Higashinari-ku, Osaka 537-8511, Japan

Edited by Ruslan Medzhitov, Yale University School of Medicine, New Haven, CT, and approved December 20, 2011 (received for review August 11, 2011)

Smoldering inflammation often increases the risk of progression for malignant tumors and simultaneously matures myeloid dendritic cells (mDCs) for cell-mediated immunity. PolyI:C, a dsRNA analog, is reported to induce inflammation and potent antitumor immune responses via the Toll-like receptor 3/Toll–IL-1 receptor domain-containing adaptor molecule 1 (TICAM-1) and melanoma differentiation-associated protein 5/IFN-β promoter stimulator 1 (IPS-1) pathways in mDCs to drive activation of natural killer cells and cytotoxic T lymphocytes. Here, we found that i.p. or s.c. injection of polyI:C to Lewis lung carcinoma tumor-implant mice resulted in tumor regression by converting tumor-supporting macrophages (Mfs) to tumor suppressors. F4/80⁺/Gr1⁻ Mfs infiltrating the tumor respond to polyI:C to rapidly produce inflammatory cytokines and thereafter accelerate M1 polarization. TNF-α was increased within 1 h in both tumor and serum upon polyI:C injection into tumor-bearing mice, followed by tumor hemorrhagic necrosis and growth suppression. These tumor responses were abolished in TNF-$\alpha^{-/-}$ mice. Furthermore, F4/80⁺ Mfs in tumors extracted from polyI:C-injected mice sustained Lewis lung carcinoma cytotoxic activity, and this activity was partly abrogated by anti–TNF-α Ab. Genes for supporting M1 polarization were subsequently up-regulated in the tumor-infiltrating Mfs. These responses were completely abrogated in TICAM-$1^{-/-}$ mice, and unaffected in myeloid differentiation factor $88^{-/-}$ and IPS-$1^{-/-}$ mice. Thus, the TICAM-1 pathway is not only important to mature mDCs for cross-priming and natural killer cell activation in the induction of tumor immunity, but also critically engaged in tumor suppression by converting tumor-supporting Mfs to those with tumoricidal properties.

Toll-like receptor | tumor-associated macrophages | TRIF

Inflammation followed by bacterial and viral infections triggers a high risk of cancer and promotes tumor development and progression (1, 2). Long-term use of anti-inflammatory drugs has been shown to reduce—if not eliminate—the risk of cancer, as demonstrated by a clinical study of aspirin and colorectal cancer occurrence (3). Inflammatory cytokines facilitate tumor progression and metastasis in most cases. Innate immune response and the following cellular events are closely concerned with the formation of the tumor microenvironment (4, 5).

By contrast, inflammation induced by microbial preparations was applied to patients with cancer for therapeutic potential as Coley vaccine with some success. A viral replication product, dsRNA and its analog polyI:C (6, 7), induced acute inflammation, and has been expected to be a promising therapeutic agent against cancer. Although polyI:C exerts life-threatening cytokinemia (8), trials for its clinical use as an adjuvant continued because of its high therapeutic potential (9, 10). Pathogen-associated molecular patterns (PAMPs) and host cell factors induced secondary to PAMP–host cell interaction act as a double-edged sword in cancer prognosis and require understanding their multifarious functional properties in the tumor environment.

Recent advances in the study of innate immunity show how polyI:C suppresses tumor progression (11). PolyI:C is a synthetic compound that serves as an agonist for pattern-recognition receptors (PRRs), Toll-like receptor 3 (TLR3), and melanoma differentiation-associated protein 5 (MDA5) (12–14). Although TLR3 and MDA5 signals are characterized as myeloid differentiation factor 88 (MyD88) independent (15, 16), they have immune effector-inducing properties (12–14, 17). TLR3 couples with the Toll–IL-1 receptor domain-containing adaptor molecule 1 (TICAM-1, also known as TRIF), and MDA5 couples with the IFN-β promoter stimulator 1 (IPS-1, also known as Cardif, MAVS, or VISA) (11, 15). Possible functions for the TICAM-1 and IPS-1 signaling pathways have been investigated by using gene-disrupted mice (15); although they activate the same downstream transcription factors NF-κB and IFN regulatory factor 3 (IRF-3) (15, 18), they appear to distinctly modulate myeloid dendritic cells (mDCs) and macrophages (Mfs) to drive effector lymphocytes (19, 20).

Tumor microenvironments frequently involve myeloid-derived suppressor cells (MDSCs), tumor-associated macrophages (TAMs), and immature mDCs (1, 21). These myeloid cells express PRR through which they are functionally activated. Once the inflammation process is triggered, immature mDCs turn mature so that they are capable of antigen cross-presentation and able to activate immune effector cells, which would act to protect the host system and damage the undesirable tumor cells (22). However, TAMs and MDSCs play a major role in establishing a favorable environment for tumor cell development by suppressing antitumor immunity and recruiting host immune cells to support tumor cell survival, motility, and invasion (23–25). Although these myeloid cell scenarios have been studied with interest, how the PRR signal in these myeloid cells links regulation of tumor progression has yet to be elucidated.

Here we show that TICAM-1 but not IPS-1 signal in tumor-infiltrating Mfs is engaged in conversion of the TAM-like Mfs to tumoricidal effectors. We investigated the molecular mechanisms in Mfs underlying the phenotype switch from tumor supporting to tumor suppressing by treating cells with polyI:C and found that the TICAM-1–inducing TNF-α and M1 polarization are crucial for eliciting tumoricidal activity in TAMs.

Results

In Vivo Effect of PolyI:C on Implant Lewis Lung Carcinoma Tumor. I.p. injection of polyI:C rapidly induced hemorrhagic necrosis in 3LL tumors implanted in WT mice, which was established >12 h after polyI:C treatment (Fig. 1*A*). The polyI:C-dependent hemorrhagic necrosis did not occur in TNF-$\alpha^{-/-}$ mice (Fig. 1*A*). Histological

Author contributions: H.S., M.M., and T.S. designed research; H.S., H.O., and S.T. performed research; H.O., A.N., Y.I., and H.T. contributed new reagents/analytic tools; M.M. and N.I. analyzed data; and H.S. and T.S. wrote the paper.

The authors declare no conflict of interest.

This article is a PNAS Direct Submission.

[1]To whom correspondence should be addressed. E-mail: seya-tu@pop.med.hokudai.ac.jp.

This article contains supporting information online at www.pnas.org/lookup/suppl/doi:10.1073/pnas.1113099109/-/DCSupplemental.

and immunohistochemical analysis revealed vascular damage in the necrotic lesion, where disruption of vascular endothelial cells was indicated by fragmented $CD31^+$ marker (Fig. S1). Although the polyI:C signal is delivered by TICAM-1 and IPS-1 adaptors (11, 13), the hemorrhagic necrosis was largely alleviated in TICAM-$1^{-/-}$ mice but not in IPS-$1^{-/-}$ mice (Fig. 1*A*). The results suggest that polyI:C is a reagent that induces Lewis lung carcinoma (3LL) hemorrhagic necrosis, and the TICAM-1 pathway and its products, including TNF-α, are preferentially involved in this response.

3LL implant tumors grew well in WT C57BL6 mice. PolyI:C, when i.p. injected, resulted in tumor growth retardation (Fig. 1*B*). The retardation of tumor growth by polyI:C was also impaired in TNF-$\alpha^{-/-}$ mice (Fig. 1*B*), suggesting that TNF-α is a critical effector for not only induction of hemorrhagic necrosis but also further 3LL tumor regression. To investigate the signaling pathway involved in the tumor growth retardation by polyI:C, we challenged WT, MyD$88^{-/-}$, TICAM-$1^{-/-}$, and IPS-$1^{-/-}$ mice with 3LL implantation and then treated the mice with i.p. injection of polyI:C. 3LL growth retardation was observed in both IPS-$1^{-/-}$ (Fig. 1*C*) and MyD$88^{-/-}$ mice, to a similar extent to WT mice. In contrast, polyI:C-dependent tumor growth retardation was abrogated in TICAM-$1^{-/-}$ mice (Fig. 1*D*). The size differences of the implanted tumors became significant within 2 d after polyI:C treatment, suggesting that the molecular effector for tumor regression is induced early and its upstream is TICAM-1. Similar results were obtained with MC38 implant tumor (Fig. S2*A*), which is TNF-α sensitive and MHC class I positive (Table S1) (26).

PolyI:C is a reagent that induces natural killer (NK) cell activation in MHC class I-negative tumors (12), and 3LL cells are class I negative and NK cell sensitive (Table S1) (27, 28). We tested whether NK cells activated by polyI:C damage the 3LL tumor in mice. Tumor growth was not affected by pretreatment of the mice with anti-NK1.1 Ab in this model (Fig. S3). Thus, NK cells, at least the NK1.1^+ cells, have a negligible ability to retard tumor growth in vivo.

PolyI:C Induces TNF-α Through the TICAM-1 Pathway in Mice. To test whether polyI:C treatment had elicited TNF-α production in vivo, we investigated the cytokine profiles of serum from polyI:C-stimulated WT and IPS-$1^{-/-}$ and TICAM-$1^{-/-}$ mice by ELISA. Prominent differences in TNF-α levels were observed in serum collected from polyI:C-injected WT and TICAM-$1^{-/-}$ mice. Serum TNF-α levels in WT and IPS-$1^{-/-}$ mice were significantly higher than that in TICAM-$1^{-/-}$ mice within 1 h after polyI:C injection (Fig. S4 *A* and *B*). IFN-β is a main output for polyI:C stimulation (11), and its production was decreased in TICAM-$1^{-/-}$ mice and totally abrogated in IPS-$1^{-/-}$ mice (Fig. S4*C*). Taken together, the data indicate that the TICAM-1 pathway was able to sustain a high TNF-α level in the early phase of polyI:C treatment, which is independent of IPS-1 and subsequent production of IFN-β.

TICAM-1⁺ Cells in Tumor Produces TNF-α in Response to PolyI:C Stimulation. Using the 3LL implant WT, IPS-$1^{-/-}$, and TICAM-$1^{-/-}$ mouse models, we tested whether polyI:C-induced early TNF-α was responsible for the lately observed tumor regression. Time-course analyses of the polyI:C-induced TNF-α protein levels were performed by ELISA using serum samples and tumors extracted from the experimental mice. The tumor TNF-α levels in WT and IPS-$1^{-/-}$ mice increased at 2 h after polyI:C i.p. injection (Fig. 2*A*). The serum TNF-α levels in both were rapidly up-regulated within 1 h after polyI:C injection, although in WT the levels continued to increase but in IPS-$1^{-/-}$ mice gradually decreased (Fig. 2*B*). In TICAM-$1^{-/-}$ mice, however, no appreciable up-regulation of TNF-α protein was detected in either tumor or serum samples during the early time-course tested. To test whether the induced TNF-α protein was generated de novo in tumors, we examined the corresponding mRNA levels in excised tumors (Fig. 2*C* and Table S2). The TNF-α mRNA levels peaked between 1 and 2 h after polyI:C injection, whereas the TNF-α protein level was kept high at >2 h after polyI:C injection in tumor as well as serum. In the TICAM-$1^{-/-}$ mice, TNF-α production was largely abrogated in the tumor and serum samples, suggesting that TNF-α was mainly produced and secreted in response to polyI:C stimulation from the TLR3/TICAM-1^+ cells within the tumor.

F4/80⁺/Gr-1⁻ Mfs in 3LL Tumor Produce TNF-α Leading to Tumor Damage. We next investigated the cell types that had infiltrated the tumor by using various Mf markers in FACS analysis and tumor samples extracted at 1 h after polyI:C injection. We discovered that $CD45^+$ cells in the tumor produced TNF-α in response to polyI:C (Fig. 3*A*). The major population of those $CD45^+$ cells was determined to be of $CD11b^+$ myeloid-lineage cells that coexpressed F4/80^+, $Gr1^+$, or $CD11c^+$. A small population of NK1.1^+ cells was also detected. $CD4^+$ T cells, $CD8^+$ T cells, and B cells were rarely detected in these implant tumors (Fig. S5*A*). Moreover, F4/80^+/Gr-1^- cells were found to be the principal contributors to polyI:C-mediated TNF-α production (Fig. 3 *B* and *C*). F4/80^+ cells in 3LL tumor highly expressed macrophage mannose receptor (MMR; CD206), a M2 macrophage marker, in contrast to splenic F4/$80^+$$CD11b^+$ cells. Both TNF-α–producing and –nonproducing F4/80^+ cell populations in 3LL tumor showed indistinguishable levels of CD206 (Fig. S6), and dissimilar to MDSCs or splenic Mfs, as determined by the surface marker profiles (Table S3). Thus, the source of the TNF-α–producing cells in tumor is likely F4/80^+ Mfs with a TAM-like feature.

We harvested F4/80^+ cells from tumor samples extracted from WT and TICAM-$1^{-/-}$ mice at 30 min after polyI:C injection. These cells were used in in vitro experiments to verify the TNF-α–producing abilities and 3LL cytotoxicity properties (Fig. 4 *A* and *B*). WT F4/80^+ Mfs exhibited normal TNF-α–producing function and were able to kill 3LL cells upon exposure. This tumoricidal activity was ~50% neutralized by the addition of anti–TNF-α Ab (Fig. 4*C*), although incomplete inhibition by this mAb may reflect participation of other factors in TNF-α cytotoxicity. Furthermore, when active TNF-α protein (rTNF-α) was added exogenously to 3LL cell culture, the cytotoxic effects were still present and occurred in a dose-dependent manner (Fig. 4*D*). TNF-α–producing ability was also observed in F4/80^+ cells from implant tumor of MC38, B16D8, or EL4, and only the MC38 tumor was remediable by TICAM-1–derived TNF-α (Fig. S2 *B* and *C*). The MC38 tumor contained the F4/80^+/$CD11b^+$/$Gr1^-$ cells, as in the 3LL tumor (Fig. S5*B*).

IFN-β did not enhance rTNF-α–mediated 3LL killing efficacy (Fig. S7*A*), a finding that was consistent with previously published data (29). No effect of IRF3/7 on polyI:C-induced 3LL tumor regression in vivo was confirmed using IRF3/7 double-knockout mice. However, polyI:C-dependent tumor regression was abrogated in 3LL-bearing IFN-α/β receptor $(IFNAR)^{-/-}$ mice (Fig. S7*B*). Quantitative PCR analysis of cells from WT vs. $IFNAR^{-/-}$ tumor-bearing mice revealed that the TLR3 level was basally low and not up-regulated in response to polyI:C in tumor-infiltrating F4/80^+ Mfs of $IFNAR^{-/-}$ mice (Fig. S7*C*). Accordingly, the TNF-α level was not up-regulated in tumor and serum in polyI:C-stimulated $IFNAR^{-/-}$ mice (Fig. S7*D*). Thus, basal induction of type I IFN serves as a critical factor for TLR3 function in tumor F4/80^+ Mfs to produce TNF-α in vivo. These results suggest that the direct effector for 3LL cytolysis by polyI:C involves TNF-α, which is derived from TICAM-1 downstream independent of the IRF3/7 axis. Our results indicate that cytotoxic TNF-α is produced via a distinct route from initial type I IFN and downstream of TICAM-1 in F4/80^+ TAM-like Mfs. Type I IFN do not synergistically act with TNF-α on 3LL killing, but is required to complete the TLR3/TICAM-1 pathway.

These results were confirmed by in vitro assay, wherein the F4/80^+ Mfs harvested from 3LL tumors in WT, TICAM-$1^{-/-}$, IPS-$1^{-/-}$, and $TLR3^{-/-}$ mice were stimulated with polyI:C (Fig. S8*A*). Both TNF-α release and 3LL cytotoxic abilities of polyI:C-stimulated F4/80^+ Mfs were specifically abrogated by the absence of TICAM-1 and TLR3 (Fig. S8 *A* and *B*). IPS-1 or

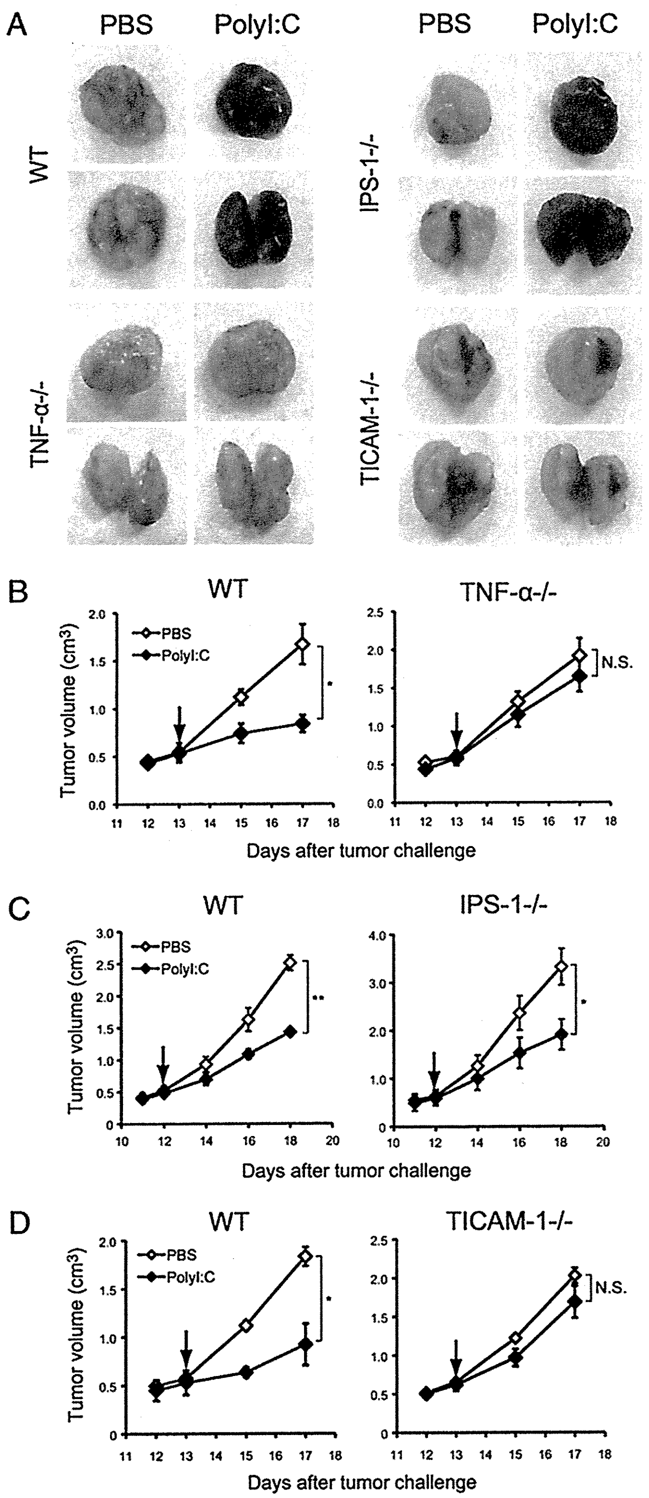

Fig. 1. Antitumor activity of polyI:C against 3LL tumor cells is mediated by the TICAM-1 pathway in vivo. (*A*) Representative photographs of 3LL tumors excised from WT, TNF-$\alpha^{-/-}$, TICAM-$1^{-/-}$, and IPS-$1^{-/-}$ mice. Whole tumor (*Upper*) and bisected tumor (*Lower*) are shown. (*B–D*) On day 0, 3LL tumor cells (3×10^6) were s.c. implanted into B6 WT (*B–D*), TNF-$\alpha^{-/-}$ (*B*), TICAM-$1^{-/-}$ (*C*), and IPS-$1^{-/-}$ (*D*) mice. PolyI:C i.p. injection was started on the day indicated by arrow, then repeated every 4 d. Data are shown as tumor average size ± SE; n = 3–4 mice per group. *$P < 0.05$; **$P < 0.001$. N.S., not significant. A representative experiment of two with similar outcomes is shown.

MyD88 in F4/80$^+$ Mfs had no or minimal effect on the TNF-α tumoricidal effect against 3LL tumors. PolyI:C did not directly exert a cytotoxic effect on 3LL tumor cells (Fig. S8*C*).

Role of the IPS-1 Pathway in F4/80$^+$ Cells. Both TICAM-1 and IPS-1 are known to converge their signals on transcription factors NF-κB and IRF-3, which drive expression of TNF-α and IFN-β, respectively. PolyI:C-induced TNF-α production was reduced in F4/80$^+$ cells extracted from tumors of TICAM-$1^{-/-}$ mice, but not in samples of IPS-$1^{-/-}$ mice. We examined the expression of IFN-β in these cells after polyI:C stimulation. Compared with F4/80$^+$ cells from WT mice, IFN-β expression and production was barely decreased in IPS-$1^{-/-}$ F4/80$^+$ cells, but largely impaired in TICAM-$1^{-/-}$ F4/80$^+$ cells (Fig. S9*A*) as other cytokines tested. M1 Mf-associated cytokines/chemokines were generally reduced in TICAM-$1^{-/-}$ F4/80$^+$ cells compared with WT and IPS-$1^{-/-}$ cells >4 h after polyI:C stimulation (Fig. S9*A*), whereas M2 Mf-associated genes were barely affected by TICAM-1 disruption or polyI:C stimulation (Fig. S9*B*).

Most types of Mfs are known to express TLR3 in mice (30). Messages and proteins for type I IFN induction were conserved in the F4/80$^+$ tumor-infiltrating Mfs (Fig. S10 *A–C*). However, the TLR3 mRNA level was low in macrophage colony-stimulating factor (M-CSF)–derived Mfs compared with TAMs (Fig. S10*D*). We further examined whether IFN-β production might also have relied on the TICAM-1 pathway in other types of Mfs upon stimulation with polyI:C. In contrast to the F4/80$^+$ cells isolated from tumor (Fig. S11*A* and *B*), the IPS-1 pathway was indispensable for polyI:C-mediated IFN-β production in mouse peritoneal Mfs and M-CSF–induced bone marrow-derived Mfs (Fig. S11 *C* and *E*). However, IPS-1 only slightly participated in polyI:C-mediated TNF-α production in these Mf subsets (Fig. S11 *D* and *F*). It appears then that the IPS-1 pathway is able to signal the presence of polyI:C and subsequently induce type I IFN. TICAM-1 is the protein that induces effective TNF-α in all subsets of Mfs.

PolyI:C Influences Polarization of TAMs. Plasticity is a characteristic feature of Mfs (25). Various factors and signals can influence polarization of Mf cells to induce the M1/M2 transition, which is accompanied by a substantial change in the Mf cell's expression profile of cytokines and chemokines. Previous studies have demonstrated that Mfs that have infiltrated into tumor are of the M2-polarized phenotype, which is known to contribute to tumor progression. To test the effects of polyI:C on the polarization of tumor-infiltrated Mf cells, we analyzed the gene expression profiles of these cells following in vitro polyI:C stimulation, and representative profiles were confirmed by quantitative PCR (Fig. 5 *A* and *B*). The mRNA expressions were increased for M1 Mf markers IL-12p40, IL-6, CXCL11, and IL-1β at 4 h after in vitro polyI:C treatment, as were mRNA levels of IFN-β and TNF-α and ex vivo results. The M2 Mf markers arginase-1 (*Arg1*), chitinase 3-like 3 (*Chi3l3*), and MMR (*Mrc1*) were unchanged, compared with unstimulated levels; however, the M2 Mf marker IL-10, a regulatory cytokine, was induced. In addition, there was no difference observed in the mRNA expression levels of MMP9 (*Mmp9*) and VEGFA (*Vegfa*), both of which are involved in tissue remodeling and angiogenesis events of tumor progression (Fig. 5*C*). The polyI:C-induced M1 markers and IL-10 expression that were up-regulated in WT and IPS-$1^{-/-}$ F4/80$^+$ cells were found to be abrogated in TICAM-$1^{-/-}$ F4/80$^+$ cells (Fig. 5*A* and *B*), reinforcing the results obtained with F4/80$^+$ Mfs isolated from 3LL tumors in mice injected with polyI:C (Fig. S9 *A* and *B*). It appears that TICAM-1 is responsible for the M1 polarization of F4/80$^+$ Mf cells in tumors, but has no effect on M2 markers. We further examined the expression of IRF-5 and IRF-4, which are considered the master regulators for M1 and M2 polarization, respectively (31, 32). As expected, polyI:C induced IRF-5 mRNA expression, but had no effect on IRF-4 mRNA expression in vitro (Fig. 5*A* and *B*). Jmjd3, a histone H3K27 demethylase involved in IRF-4 expression, is reportedly induced by TLR stimulation (33). In our study, polyI:C stimulation increased Jmjd3 mRNA in F4/80$^+$ cells

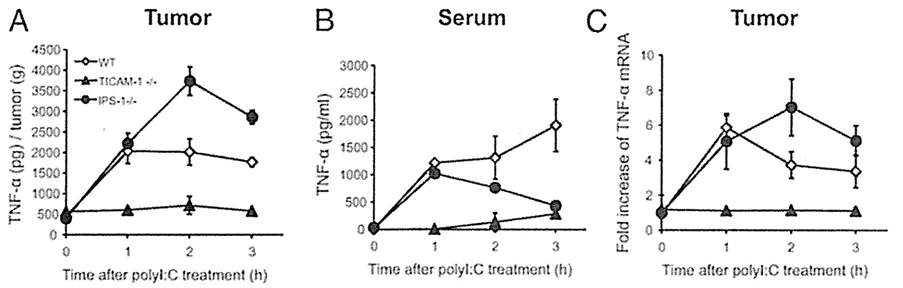

Fig. 2. TNF-α production in tumor and serum of polyI:C-injected 3LL tumor-bearing mice. Mice bearing 3LL tumor were i.p. injected with 200 μg polyI:C. Tumor (*A*) and serum (*B*) were collected at 0, 1, 2, and 3 h after polyI:C injection, and TNF-α concentration was determined by ELISA. TNF-α level in tumor is presented as [TNF-α protein (pg)/tumor weight (g)]. (*C*) Tumors were isolated from polyI:C-injected tumor-bearing WT, TICAM-$1^{-/-}$, and IPS-$1^{-/-}$ mice, and TNF-α mRNA was measured by quantitative PCR; $n = 3$. Data are shown as average ± SD. A representative experiment of two with similar outcomes is shown.

(Fig. 5*B*). The polyI:C-triggered M1 gene expression continued long in tumor-infiltrated Mfs, a finding that may further explain the tumor-suppressing feature of these Mfs, in addition to the concern of early inducing TNF-α.

Discussion

In this study we demonstrated that the tumor-supporting properties of tumor-infiltrating F4/80$^+$ Mfs characterized by M2 markers are dynamic and able to shift to an M1-dominant state upon the particular signal provided by PRRs. In 3LL tumors that express minimal amounts of MHC class I/II and recruit a large amount of myeloid cells, F4/80$^+$ Mfs function to sustain the tumor in the surrounding microenvironment. This tumor-supporting environment can be disrupted by stimulation with an RNA duplex through a TICAM-1 signal and subsequent induction of mediators such as TNF-α. Thus, the TICAM-1 signal in tumor-infiltrating Mfs plays a key role in TNF-α and M1 shift-mediated tumor regression. These results were confirmed using another cell line, MC38 colon adenocarcinoma (34), although MC38 cells express MHC class I. B16D8 melanoma (12) and EL4 lymphoma (35) were resistant to TNF-α, but their F4/80$^+$ Mfs still possessed TNF-α–inducing potential by stimulation with polyI:C; their susceptibilities to polyI:C reportedly depend on other effectors (12, 35). These results may partly explain the reported findings that tumors regressed in patients with simultaneous virus infection (36, 37), and that tumor growth was inhibited by polyI:C injection in tumor-bearing mice (6, 7).

In contrast, polyI:C-stimulated PEC or bone marrow-derived Mfs induce type I IFN via the IPS-1 pathway unlike the case of tumor-infiltrating F4/80$^+$ Mfs. Nevertheless, all of these Mf subsets produce proinflammatory cytokines, including TNF-α, in a TICAM-1–dependent manner. Thus, the key question that arose was why predominant TICAM-1 dependence for polyI:C-mediated production of TNF-α occurred in F4/80$^+$ tumor-infiltrating Mfs leading to tumor regression. A marked finding is that the TLR3 protein level is high in tumor-infiltrating Mfs compared with other sources of Mfs (Fig. S10). In addition, the IPS-1 pathway is unresponsive to polyI:C if the polyI:C is exogenously added to the tumor-infiltrating Mfs without transfection reagents. The cytoplasmic dsRNA sensors normally work for IFN induction in tumor F4/80$^+$ Mfs if the polyI:C is transfected into the cells. TICAM-1–dependent TNF-α production by F4/80$^+$ Mfs (Fig. S11 *D* and *F*) occurs partly because F4/80$^+$ Mfs express a high basal level of TLR3 and fail to take up extrinsic polyI:C into the cytoplasm. Of many subsets of Mfs, these properties (38) are unique to the F4/80$^+$ Mfs.

Hemorrhagic necrosis and tumor size reduction are closely correlated with constitutive production of TNF-α (39, 40). The association of PRR-derived TNF-α and hemorrhagic necrosis of tumor has been described earlier. Carswell et al. (41) showed that TNF-α is robustly expressed in mouse serum following treatment with bacillus Calmette–Guérin and endotoxin. Bioassay of TNF-α as reflected by the degree of hemorrhagic necrosis of transplanted Meth A sarcoma in BALB/c mice led the authors to speculate that Mfs are responsible for TNF-α induction. Many years later, Dougherty et al. (42) identified the mechanism responsible for the TNF-α production associated with antitumor activity; macrophages isolated from tumors in mice with inactivating mutation in the TLR4 gene [Lps(d) in C3H/HeJ] expressed 5- to 10-fold less TNF-α than tumors in WT mice. This finding represents a unique recognition of a PRR contributing to the cancer phenotype. Subsequent studies determined that MyD88 is involved in the induction of TNF-α via TLR4 binding to its cognate ligand, lipid A endotoxin (15, 43). Because the TLR3 signal is independent of MyD88, this MyD88 concept is not applicable to the present study on polyI:C-dependent tumor regression.

Alternatively, endotoxin/lipid A may have activated TICAM-1 in previous reports on TLR4-derived TNF-α because TLR4 can recruit TICAM-1 in addition to MyD88 (15). The lipid A derivative monophospholipid A preferentially activates the TICAM-1 pathway of TLR4 (43). It is likely that TICAM-1 participates in TLR4-mediated tumor regression in addition to MyD88, although MyD88 is not involved in the polyI:C signaling. This point was further proven using TNF-$\alpha^{-/-}$ mice: TICAM-1-derived TNF-α in F4/80$^+$ Mf cells has a critical role in the induction of tumor necrosis and regression by polyI:C. The results are consistent with the finding that both TICAM-1 and IPS-1 pathways are able to induce NF-κB activation secondary to polyI:C stimulation, and indeed their signals converge at the IκB kinase complex (18).

TICAM-1 is able to induce many of the IFN-inducible genes that MyD88 cannot in mDCs (44). In both cases of TICAM-1 and MyD88 stimulation, tumor-infiltrating Mfs facilitate the expression of many genes in addition to TNF-α. The M2 phenotype of F4/80$^+$ Mfs or tumor-associated Mfs is modified dependent on these additional factors. IFNAR facilitates polyI:C-mediated tumor regression in tumor-bearing mice, lack of which results in no induction of TLR3 (Fig. S7). Thus, preceding the polyI:C

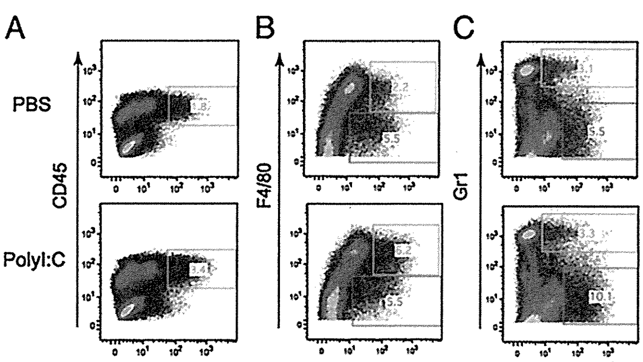

Fig. 3. F4/80$^+$ cells are responsible for the polyI:C-induced elevation of TNF-α production in tumor. Mice bearing 3LL tumors were i.p. injected with 200 μg polyI:C. TNF-α–producing cells in tumors of polyI:C- or PBS-injected mice were examined by immunohistochemical staining and flow cytometry to determine intracellular cytokine expression profiles of CD45$^+$ cells (*A*), F4/80$^+$ cells (*B*), and Gr1$^+$ cells (*C*). CD45$^+$ cells in tumor were gated and are shown in *B* and *C*. A representative experiment of two with similar outcomes is shown. TNF-α$^+$ gating squares are shown in red (positive) and green (negative).